

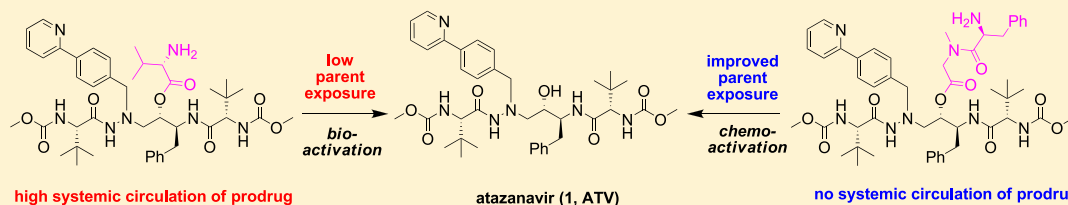
Design, Synthesis, and Pharmacokinetic Evaluation of Phosphate and Amino Acid Ester Prodrugs for Improving the Oral Bioavailability of the HIV-1 Protease Inhibitor Atazanavir

Murugaiah A. M. Subbaiah,^{*,†} Sandhya Mandlekar,[§] Sridhar Desikan,^{‡,∇} Thangeswaran Ramar,[†] Lakshumanan Subramani,[†] Mathiazhagan Annadurai,[†] Salil D. Desai,[‡] Sarmistha Sinha,[§] Susan M. Jenkins,^{#,¶} Mark R. Krystal,^{1,¶} Murali Subramanian,[§] Srikanth Sridhar,[‡] Shweta Padmanabhan,[§] Priyadeep Bhutani,[§] Rambabu Arla,[§] Shashyendra Singh,[§] Jaydeep Sinha,[§] Megha Thakur,[§] John F. Kadow,^{1,¶} and Nicholas A. Meanwell^{1||}

[†]Department of Medicinal Chemistry, [‡]Department of Biopharmaceutics, and [§]Department of Pharmaceutical Candidate Optimization, Biocon-Bristol Myers Squibb R&D Centre, Biocon Park, Bommasandra IV Phase, Jigani Link Road, Bangalore 560099, India

^{||}Department of Discovery Chemistry and Molecular Technologies, ¹Department of Virology, and [#]Department of Pharmaceutical Candidate Optimization, Bristol-Myers Squibb Research and Development, P.O. Box 4000, Princeton, New Jersey 08543-4000, United States

S Supporting Information



ABSTRACT: Phosphate and amino acid prodrugs of the HIV-1 protease inhibitor (PI) atazanavir (**1**) were prepared and evaluated to address solubility and absorption limitations. While the phosphate prodrug failed to release **1** in rats, the introduction of a methylene spacer facilitated prodrug activation, but parent exposure was lower than that following direct administration of **1**. Val amino acid and Val-Val dipeptides imparted low plasma exposure of the parent, although the exposure of the prodrugs was high, reflecting good absorption. Screening of additional amino acids resulted in the identification of an L-Phe ester that offered an improved exposure of **1** and reduced levels of the circulating prodrug. Further molecular editing focusing on the linker design culminated in the discovery of the self-immolative L-Phe-Sar dipeptide derivative **74** that gave four-fold improved AUC and eight-fold higher C_{trough} values of **1** compared with oral administration of the drug itself, demonstrating a successful prodrug approach to the oral delivery of **1**.

INTRODUCTION

Combination antiretroviral therapy (cART), which is composed of HIV-1 inhibitors that target different aspects of the virus life cycle, is presently the most effective treatment for HIV-1 infection.¹ These drug combinations, which include inhibitors of HIV-1 protease, integrase, and reverse transcriptase (nucleoside reverse transcriptase inhibitors (NRTIs) and non-nucleoside reverse transcriptase inhibitors (NNRTIs)), have transformed HIV-1 infection from a fatal diagnosis to a manageable chronic condition, resulting in a substantial enhancement of both life expectancy and quality for most patients.² Therapy with cART usually results in long-lasting suppression of viremia to undetectable levels that translates into a restoration of CD4 counts. HIV-1 PIs, which are in most cases used in combination with a pharmacokinetic (PK) enhancer that acts by inhibiting cytochrome P450 (CYP) enzymes, have played a critical role in the evolution of cART

based on their efficacy and high genetic barrier toward the development of resistance.^{3–5} Atazanavir (ATV, **1**) is an azapeptide-based PI that received marketing authorization by the US Federal Drug Administration (FDA) in 2003 and is a designated member of the WHO list of essential medicines.⁶ It is one of the nine PIs and one prodrug that have been granted marketing authorization by the FDA.^{4,7} Although **1** is available as a monotherapeutic agent for once daily (quaque die, QD) dosing, it is typically used in conjunction with a PK enhancer as a fixed-dose combination with either ritonavir [RTV, **3**] or, more recently, cobicistat that allows for a reduced dose of the PI while maintaining target C_{trough} levels.⁸ The profile of **1** offers additional advantages over other PIs, including a more beneficial effect on lipid profiles and a low capsule burden;

Received: January 1, 2019

however, **1** brings its own side effect profile which includes hyperbilirubinemia.⁶ As part of a class effect, **1** is known for modest oral bioavailability, with ~79% of administered radioactivity recovered in the feces of humans, suggesting incomplete absorption and/or biliary excretion of the drug. This is reflected in the PK profile of **1** in preclinical species which exhibits 15% oral bioavailability in rats when dosed as a suspension and 36% in dogs from a capsule formulation.⁶ Similar to the observation in humans, the recovery of the unchanged drug from the feces was significant in both the rat (39%) and dog (79%) following oral administration. This profile can be attributed to suboptimal physicochemical properties that contribute to poor absorption and the susceptibility of **1** to metabolic modification, particularly by CYP3A4. Most prominently, **1** is characterized by poor aqueous solubility at higher pH values, modest absorptive permeability, high secretory efflux,⁹ and, importantly, an extensive first-pass metabolism. Being a weak base, **1** shows high solubility at pH = 1.0 (relevant for dissolution in the stomach) but poor solubility at pH = 6.5 (relevant for solubility and absorption in the intestine), data captured in Table 1. Following administration of a combination of **1** and **3**

Table 1. Physicochemical Properties and PK Profiling of **1**^{6,16,17}

parameter	value
molecular weight ^a	704.86
clog <i>D</i> ^a	4.54
hydrogen-bond donor (HBD) count ^a	5
hydrogen-bond acceptor (HBA) count ^a	13
rotatable bond count ^a	18
polar surface area (PSA) ^a	171 Å ²
p <i>K</i> _a ¹⁷	4.7
aqueous solubility at 25 °C ^b	pH 1.0 = 1.69 mg/mL pH 3.0 = 0.028 mg/mL pH 4.0 = <0.001 mg/mL pH 5.0 = <0.001 mg/mL pH 6.5 = <0.001 mg/mL pH 7.4 = <0.001 mg/mL
unbuffered aqueous solubility at 25 °C ^b	<0.001 mg/mL
Caco-2 permeability <i>P</i> _{app} ^b	A–B = <15 nm/s B–A = 470 nm/s efflux ratio: >31
<i>t</i> _{1/2} in rat hepatocytes ^b	27 min
absolute bioavailability ⁶	rat: 15% dog: 36%

^aPhysical properties calculated using ChemAxon Marvin Sketch software. ^bData generated in-house.¹⁶

with a 40 mg dose of a proton pump inhibitor (PPI), the exposure of **1** was reduced by 75%, demonstrating the dependence of the absorption of **1** on gut pH.^{10–12} Because of this pH effect on absorption, the use of histamine H₂ antagonists and PPIs, stomach acid modifiers that raise gastric pH, in conjunction with **1** requires caution, which can lead to reduced patient compliance. The pH-dependent absorption complicates inclusion of **1** in fixed-dose combination regimens, thereby reducing the clinical utility of the drug. Clinically, **1** is co-administered with a PK enhancer which suppresses metabolic degradation by inhibiting CYP3A enzymes. This approach facilitates an improved PK profile with higher oral bioavailability, a longer plasma *t*_{1/2}, and a higher plasma trough

concentration of **1** than in the absence of the PK enhancer and allows for a QD rather than a twice daily (bis in die, BID) dosing schedule at the preferred dose.¹³ However, this also results in additional drug–drug interactions and related toxicities, which can also contribute to reduced patient compliance.

The consequences of the high excipient loading and pill burden associated with higher doses of **1** and the need for a PK enhancer inspired a feasibility study toward the development of prodrug approaches designed to improve the systemic delivery of **1**.¹⁶ In the context of a contemporary scenario that reflects limited drug discovery effort by the pharmaceutical industry to develop next-generation PIs with enhanced PK properties and improved resistance and safety profiles,^{4,5} a strategy of improving the absorption, distribution, metabolism, and excretion (ADME) properties of existing PIs via formulation, prodrug, and other approaches assumes significance.^{18–23} For example, deuterated analogues of **1**, which were prepared by replacing hydrogen atoms with deuterium isotopes at one or more sites, including those susceptible to metabolic modification, have been investigated as a means of enhancing metabolic stability.^{24,25} However, this approach, which takes advantage of the kinetic isotope effect to slow or redirect metabolism, resulted in only a marginal improvement in oral bioavailability, failing to provide a compound amenable to single pill combination regimens while also not addressing the pH-dependent absorption issue associated with **1**.²⁵ In spite of a growing interest in the exploration of prodrugs among all therapeutic classes,^{26–29} a prodrug approach has only rarely been investigated as a means of improving the PK profile of **1**.^{16,23} The discovery of a prodrug that would demonstrate improved oral exposure of **1** and potentially eliminate the requirement for the PK enhancer would represent a significant advancement for this antiviral agent.

RESULTS AND DISCUSSION

We report herein the synthesis and evaluation of a series of phosphate- and amino acid ester-based prodrugs of **1** in an attempt to identify compounds that would confer an improved ADME profile. To the best of our knowledge, these prodrugs have never been investigated for **1**, although phosphate- and amino acid-based prodrugs have been explored with other PIs.²² We have previously described a conjugative acyl migration prodrug approach that improved the oral delivery of **1** by relying upon the sequential enzyme-mediated release of an amine that was specifically designed to trigger an intramolecular acyl migration to deliver the parent drug.¹⁶ This approach was shown to enable enhanced exposure of **1** based on improved ADME properties by relying upon a sustained release of drug from the prodrug in vivo whilst also mitigating the pH-dependent absorption associated with **1**. As part of that initiative to identify effective prodrugs of **1**, we were particularly interested in prodrugs that could be derived in a more straightforward fashion from the parent drug itself by taking advantage of the secondary alcohol moiety, a transition state-mimicking pharmacophore, as a prodrug handle.²² The design consideration behind the selection of phosphate and amino acid promoieties was based on the physiological relevance and acceptable toxicological profile of these entities. The desired characteristics of a lead prodrug would broadly include (1) acceptable aqueous buffer stability and solubility at pH = 6.5 and 7.4; (2) enhanced absorptive flux; (3) reduced secretory efflux; (4) reduced metabolic clearance associated

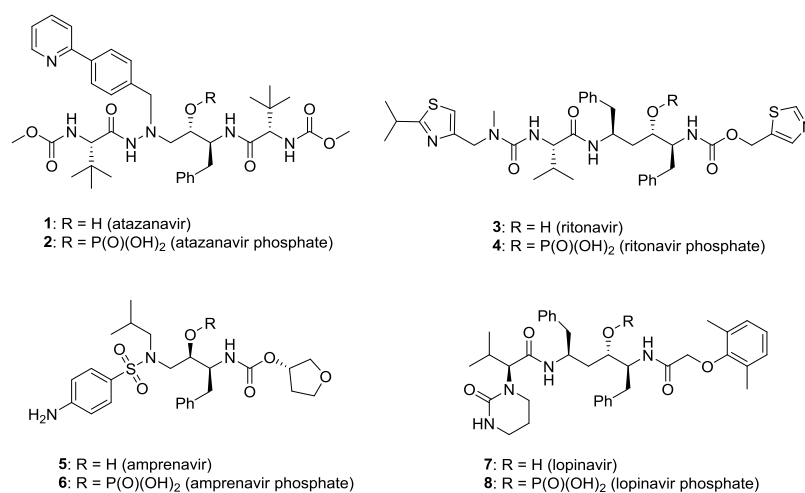
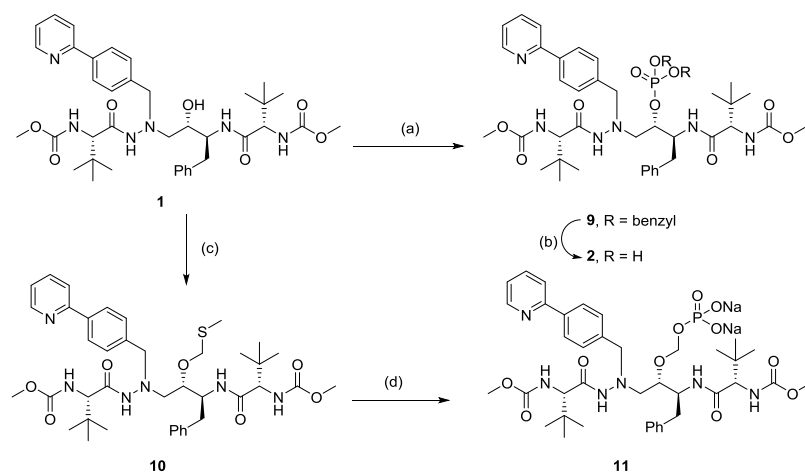


Figure 1. Structures of PIs 1, 3, 5, and 7 and their direct phosphate prodrugs (2 is described in this article; 4, 6, and 8 have been reported in the literature^{14,15}).

Scheme 1. Synthesis of Direct (2) and Methylene-Bridged (11) Phosphate-Based Prodrugs of 1^a



^aReagents and conditions: (a) dibenzyl *N,N*-diisopropylphosphoramidite, 1*H*-tetrazole (0.4 M in CH₃CN), CH₂Cl₂, RT, 8 h, then 30% aqueous H₂O₂ solution, 62%; (b) CF₃CO₂H, anisole, ClCH₂CH₂Cl, 0 °C to RT, 16 h, 72%; (c) Ac₂O, AcOH, dimethyl sulfoxide (DMSO), RT 48 h, 79%; (d) *N*-iodosuccinimide, H₃PO₄, 4 Å molecular sieves, tetrahydrofuran (THF), 0 °C to RT, 30 min, then CH₃OH, 1 M Na₂S₂O₃, Na₂CO₃ (solid), 45%.

with unproductive metabolic pathways other than prodrug release; (5) quantitative bioconversion to the parent to maximize drug exposure that also embraces the potential for a sustained release of parent drug due to a slow rate of cleavage such that the prodrug acts as a depot;¹⁶ and (6) an acceptable in vivo toxicological profile for the prodrug, the released prodrugs and the byproducts.

As a potential approach to solving the pharmaceutical issues associated with the inherently poor aqueous solubility of 1 that result in dissolution-limited and pH-dependent absorption, the initial focus was directed toward the synthesis of phosphate derivatives, with the direct phosphate prodrug 2 selected as the first iteration.^{30–37} This prodrug was designed to enhance the solubility of the drug in the gastrointestinal tract, with the release of the parent drug and nontoxic inorganic phosphate as a byproduct through a presystemic activation mechanism mediated by alkaline phosphatases (ALPs) that are abundantly expressed on the brush border membranes of enterocytes.^{30–32} While direct phosphate derivatives of 1 have not been described, phosphate monoesters of structural analogues of

1, which are covalently modified by the attachment of water-soluble nonpeptidic oligomers, have been reported.³³ Phosphate prodrugs have been investigated for other marketed PIs including 3, amprenavir (APV; 5), and lopinavir (LPV, 7), which are compounds 4, 6, and 8, respectively, with fosamprenavir (6) approved by the FDA (Figure 1).^{14,15} Fosamprenavir (6) was designed as a solubility-enhancing phosphate prodrug of 5 with the objective of allowing formulation of the molecule with a reduced excipient-to-drug ratio, thereby decreasing the high pill burden associated with 5 and providing a more patient-compliant regimen.¹⁴ The direct phosphate prodrug 2 was prepared from 1 in two synthetic steps that involved derivatization of the alcohol moiety with dibenzyl *N,N*-diisopropylphosphoramidite followed by oxidation with H₂O₂ to afford the dibenzylphosphate intermediate 9 (Scheme 1). Unmasking of the phosphate moiety by *O*-debenzylation using Pd/C-mediated hydrogenolysis was found to be cumbersome because of the concurrent cleavage of the *N*-4-(pyridin-2-yl)benzyl moiety of the parent. However, this was resolved by exposing 9 to CF₃CO₂H in the presence of

Table 2. Aqueous Stability and Solubility Data of **1** and Its Prodrugs in the pH Range of 1–6.5^a

compound #	prodrug moiety	clog <i>D</i> (pH 6.5) ^b	stability (<i>t</i> _{1/2} , h) at 37 °C			solubility (mg/mL) at 25 °C		
			pH 1	pH 4	pH 6.5	pH 1	pH 4	pH 6.5
1		4.5	ND	ND	ND	1.69	<0.001	<0.001
2	phosphate	1.6	334.3	334.3	250	>2.65	0.25	>2.87
11	POM	1.8	0.2	>500	>500	ND	>0.93	>1.06
23	L-Val	4.5	>500	376.3	334.3	>1.39	>1.58	0.5
24	D-Val	4.5	>500	>500	>500	>1.71	>1.95	0.67
29	L-Val-L-Val-1	3.9	>500	>500	>500	>2.15	>1.2	0.78
30	D-Val-D-Val-1	3.9	>500	>500	>500	>2.4	>2.2	0.82
31	D-Val-L-Val-1	3.9	>500	>500	>500	>2.0	>2.0	0.62
32	L-Val-D-Val-1	3.9	>500	>500	>500	>1.71	>1.42	0.93
44	Gly	3.4	>500	>500	39.09 ^c	>1.2	>1.6	0.96 ^c
45	Sar	4.2	>500	>334.3	25	>2.2	>2.4	0.93
46	<i>N,N</i> -dimethyl-Gly	4.5	>500	>500	188 ^c	>1.4	>1.7	0.36 ^c
47	L-Ala	3.7	>500	>500	37.6	>1.3	>1.1	0.75
48	D-Ala	3.7	>500	>500	37.6	>1.3	>1.7	0.52
49	L-Leu	4.9	>500	>500	71.6 ^c	>0.45	>0.67	0.001 ^c
50	D-Leu	4.9	>500	>500	ND	>0.66	>0.62	0.041 ^c
51	L-Met	4.4	>500	>500	103.8 ^c	>1.63	>1.53	0.044 ^c
52	D-Met	4.4	>500	>500	97.1 ^c	>0.99	>0.89	0.045 ^c
53	L-Phe	5.7	>500	>500	>500	>1.5	>1.1	0.027
54	D-Phe	5.7	>500	>500	>500	>1.2	>1.2	<0.001
59	L-Tyr	5.4	>500	376.3	214.9 ^c	>0.98	>1.42	0.009 ^c
64	L-F-Phe	5.8	>500	>500	334.3 ^c	>1.38	>0.98	<0.001 ^c
66	L-Trp	5.8	376.3	376.3	167.2 ^c	>1.04	>0.91	0.001 ^c
71	<i>N</i> -BnGly	6.1	>500	>500	334.3	>0.99	>0.71	<0.001
72	L-Phe-Gly-1	3.7	>500	>500	73.4	>2.9	>3.5	>0.64
74	L-Phe-Sar-1	3.9	>500	9.03	0.08	1.17	ND	ND
78	D-Phe-Gly-1	3.9	>500	>500	88.5	>2.1	>2.3	0.23
81	<i>N</i> -Me-L-Phe-Sar-1	3.7	376.3	15.6	0.08	>2.7	ND	ND
82	<i>N,N</i> -dimethyl-L-Phe Sar-1	5.1	376.3	>500	>334.3	>1.2	>2.2	0.02

^aFor stability studies, 30% CH₃CN in buffer was used. Buffers used were 0.1 N aqueous HCl (pH = 1.0), acetate buffer (pH = 4.0), and phosphate buffer (pH = 6.5/7.4) at a concentration of 50 mM. ND = not determined. ^bclog *D* values were calculated using ChemAxon Marvin Sketch software. ^cpH = 7.4.

anisole which facilitated selective *O*-debenzylation to afford **2**. Attempts to derive **2** directly from **1** in a single step using POCl₃ were not successful because of the absence of an isolable product.

For prodrug evaluation, we followed a simple, two-level screening tier that is composed of the determination of aqueous solution solubility and stability over the pH range of 1–6.5 followed by an *in vivo* PK evaluation in Sprague-Dawley (SD) rats involving oral administration of the prodrug at a 3 mg/kg-equivalent dose of **1**. Both the parent drug **1** and the prodrugs were formulated as solutions for dosing to rats to mitigate any potential impact of dissolution on the oral exposure. The phosphate monoester **2** showed high chemical stability, with a half-life of at least 250 h over the pH range of 1–6.5 (Table 2). In contrast to the pH-dependent solubility associated with **1**, compound **2** showed good aqueous solubility across the pH range of 1–6.5, with a ~250- and ~2800-fold improved aqueous solubility at pH = 4 and 6.5, respectively, compared with **1**. The enhanced solubility profile at the higher pH of 6.5 is especially suited to mitigating the pH-dependent intestinal absorption of **1**. However, **2** failed to deliver measurable levels of **1** in the plasma of SD rats following oral administration, in spite of the enhanced aqueous solubility. Systemic levels of circulating prodrug were negligible, an observation that can be attributed to the poor passive permeability of the highly ionized phosphate pro-

moiety at intestinal pH. To understand this *in vivo* outcome in rats, **2** was incubated with recombinant rat intestinal ALP (rIALP) with the result that negligible dephosphorylative turnover was observed within the incubation period of 120 min. Moreover, **2** was not susceptible to phosphate cleavage in the presence of human rIALP. On the basis of these *in vitro* results, the *in vivo* observation of the lack of systemic exposure of **1** from phosphate **2** can be attributed to its inefficient bioconversion to the parent drug in the intestine. To gain further insights into the structural impact of **2** on activation by ALP, rates of conversion of direct phosphate prodrugs of other PIs including **4**, **6**, and **8** were considered for a comparative review. Fosamprenavir (**6**) has been shown to undergo a high turnover in the ALP assay (*t*_{1/2} = 13.2 min) and also furnishes systemic exposure of **5** (APV) following oral administration to rats (Table 3).¹⁵ In contrast, the direct phosphate derivatives **4** and **8** of the PIs **3** and **7**, respectively, were not substrates for ALP-mediated dephosphorylation *in vitro* and **4** failed to furnish detectable systemic levels of **3** in rats following oral administration. An inspection of the structures of these prodrugs reveals a differentiated architecture associated with **6** that presumably facilitates its recognition by ALP enzymes when compared with the phosphates of the other PIs that include **1** (Figure 1). The peptidomimetic core of **1**, which closely resembles that of **3** and **7**, represents a pseudo-C₂-symmetric carboxamide-based, dipeptide isostere with an (*S*)-

Table 3. Comparison of in Vitro ALP-Mediated Cleavage Half-Life Data and Key Structural Features of Reported Phosphate Prodrugs of HIV-1 PIs with That of the Prodrugs 2 and 11 from the Parent Drug 1^a

compound #	$t_{1/2}$ in rat rIALP	$t_{1/2}$ in human rIALP	stereochemistry of OH	spacer	parent exposure in PK study
6	NT ^{b,c}		S	none	no
7	13.2 min ^{b,c}		R	none	yes
8	NT ^{b,c}		S	none	no
2	>120 min (NT) ^d	>120 min (NT) ^d	S	none	no
11	>10 min ^d	21 min ^d	S	CH ₂	yes

^aNT: no turnover of dephosphorylation. ^bReported in the literature ref 15. ^cCalf intestinal ALP. ^dData are reported in the mean of triplicates (CV < 10%).

stereochemistry of the pharmacophoric secondary hydroxyl moiety.¹⁵ In contrast, the peptidomimetic skeleton of **5** represents a sulfonamide-based dipeptide isostere with an (*R*)-configuration of the secondary alcohol. Thus, the accessibility of the promoiety groups of **2**, **4**, and **8** by ALP compared with **6** may differ significantly because of the differences in both the stereochemistry of the secondary alcohol and the P2' amide structure in the vicinity of the phosphate ester moiety. On the basis of the experimental data obtained with **2** and structural comparisons with **4** and **8**, it can be concluded that unfavorable steric features around the phosphate of **2** prevented it from effectively engaging with the active site of ALP in a fashion that allows the enzymatic dephosphorylation to proceed with efficiency.

The failure of phosphate **2** to undergo cleavage by ALP and the insights gleaned into the potential steric issues underlying these observations inspired the design of the homologue **11**, which involved the installation of a methylene spacer between **1** and the phosphate in an effort to project the site of cleavage further away from the peptidomimetic core and reduce the steric encumbrance that presumably compromises recognition by ALP. The phosphonooxymethyl (POM) prodrug **11** was envisaged to undergo presystemic dephosphorylation to release an unstable *O*-hydroxymethyl intermediate that would degrade to **1** with the extrusion of formaldehyde.³⁴ This acetal-linked prodrug strategy was given consideration, in part, based on the observation that POM prodrugs of **3** and **7** have been reported to release their parent drugs in vivo in the rat and dog.^{15,31} The POM prodrug **11** was synthesized in two steps from **1**, as depicted in Scheme 1. The first step involved the conversion of **1** into the corresponding *O*-methylthiomethyl ether **10** through a Pummerer-type rearrangement accomplished by treatment with DMSO and Ac₂O.³⁵ The second step involved the conversion of **10** to **11** through an *N*-iodosuccinimide-mediated nucleophilic displacement with orthophosphoric acid that was conducted in the presence of 4 Å molecular sieves (Scheme 1).¹⁵ Because phosphate **11** was found to be somewhat unstable in the free acid form, it was isolated as its disodium salt by adding Na₂CO₃ at the completion of the reaction and purifying the crude product using buffer-free, reversed-phase high-performance liquid chromatography (HPLC). Phosphate **11** exhibited poor chemical stability at low pH ($t_{1/2}$ = 12 min and 1.95 h at pH values of 1 and 2,

respectively) and robust stability with elevated pH ($t_{1/2}$ > 500 h at pH values of 4 and 6.5) (Table 2). The solution stability profile of **11** suggests that the POM moiety may degrade to some extent in the stomach but will be more stable in the intestine. Prodrug **11** displayed >900-fold improved solubility compared with **1** at pH values of 4 and 6.5. Following oral administration to SD rats, the prodrug was found to release the parent in vivo, providing systemic exposure of **1** that was only slightly lower than that following direct administration of **1** in a precipitation-resistant formulation. The relative oral bioavailability of **1** after dosing of **11** was 72% (Table 4) while systemic circulation of **11** was found to be negligible, results that are consistent with cleavage of the POM prodrug at the brush border membrane of the intestinal mucosa prior to absorption. Following incubation with rat rIALP, prodrug **11** was found to undergo rapid enzyme-mediated cleavage to give **1**, with the $t_{1/2}$ value of less than 10 min (Table 3). In human rIALP, the cleavage half-life was 21 min, indicative of a slower rate of dephosphorylation compared with the rat enzyme. On the basis of the in vitro solubility and in vivo PK profiles, the POM prodrug in **11** appears to be a useful approach to mitigate the solubility-related pharmaceutical issues associated with **1**. However, it may also be inferred from the PK data that enhanced solubility alone cannot substantially increase the oral exposure of **1** if there exists a significant role for efflux and metabolism in influencing oral bioavailability. As a class, orally administered phosphate prodrugs may not be able to modulate the barriers of efflux and metabolism because of the lack of transcellular passive absorption associated with the presence of the polar ionized promoiety.^{36,37}

Considering the limitations associated with the phosphate prodrugs **2** and **11**, the next phase of prodrug synthesis was directed toward the design of amino acid-based prodrugs. In light of the ALP-mediated activation challenges associated with the direct phosphate prodrug **2**, a critical element was to develop an understanding of whether direct amino acid prodrugs could undergo enzyme-mediated activation in vivo and further enhance the oral exposure of **1**. Amino acid ester prodrugs, which can undergo proteolytic cleavage by a number of specific and nonspecific esterases and peptidases found in the stomach, intestine, liver, and plasma, have found wide application across drug classes and therapeutic areas.^{27,28,38} Natural amino acids and their metabolites are useful promoiety because they are ubiquitous in the human body and their release in vivo may not pose a significant safety hazard. This kind of prodrug derivatization has been shown to improve aqueous solubility, enhance membrane permeability, modulate metabolic disposition and, in some cases, demonstrate prolonged release of the parent drug in vivo.^{38,39} Some amino acid-based prodrugs have shown to improve intestinal absorption by taking advantage of active transport processes that can enhance the oral exposure of poorly permeable drugs, exemplified most effectively by valacyclovir (**13**) and valganciclovir (**15**), clinically successful prodrugs of acyclovir (**12**) and ganciclovir (**14**), respectively. In the case of **13** and **15**, the enhanced exposure can potentially be attributed to active transport mediated by oligopeptide transporters that includes the proton-coupled peptide transporter 1 (PepT1) expressed in the brush-border membrane of intestinal mucosa and/or reduced efflux associated with a lower affinity of the prodrugs to efflux transporters like P-glycoprotein (P-gp).⁴⁰

Design considerations involving the precedent of Val-based prodrugs **13** and **15** and previous exploration of the Val

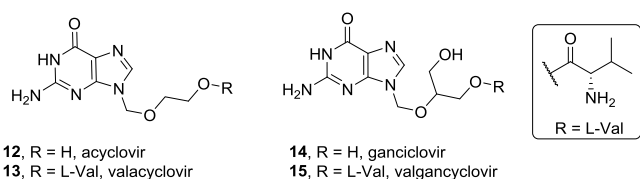
Table 4. PK Data in SD Rats Obtained after Oral Administration of **1** at 3 mg/kg and Selected Prodrugs at an Equivalent Dose of 3 mg/kg of the Parent Drug^a

compound dosed	promoiety	analyte	C _{max} (nM)	t _{max} (h)	AUC _{last} (nM h)	relative ATV AUC from the prodrug (%)	relative total AUC (prodrug + parent) (fold change)	prodrug/parent ratio
1		1	266	0.5	384 ^b		NA	
11	POM	1	257	0.25	277	72	0.72	NA
		11	NA	NA	BLQ			
23	L-Val	1	10	1.7	42	11	12.4	113
		23	1529	0.5	4731			
24	D-Val	1	6	1.5	23	6	10.1	167
		24	990	0.6	3845			
29	L-Val-L-Val-1	1	4	5.0	20	5	9.6 ^c	184 ^c
		23	30	3.0	85			
		29	1179	3.0	3598			
30	D-Val-D-Val-1	1	12	1.0	53	14	13.9 ^c	99 ^c
		24	1430	0.5	4894			
		30	384	0.3	374			
44	Gly	1	162	9.0	224	58	1.84	2.2
		44	617	1.3	484			
45	Sar	1	9.0	0.5	29.6	8	0.14	0.8
		45	8.9	0.8	23.7			
46	N,N-dimethyl-Gly	1	66.8	0.3	45.7	12	4.10	33.2
		46	1407	0.3	1519			
47	L-Ala	1	39	3	94	24	1.35	4.5
		47	235	2	423			
48	D-Ala	1	3	4.3	8	2	0.23	10.3
		48	52	1.8	82			
49	L-Leu	1	72	0.5	130	34	1.40	3.1
		49	241	0.5	406			
51	L-Met	1	37	0.83	53	14	0.37	1.7
		51	73	0.42	90			
53	L-Phe	1	456	0.5	573	149	3.28	1.2
		53	474	0.5	686			
54	D-Phe	1	64	0.5	154	40	4.50	10.2
		54	649	0.33	1575			
59	L-Tyr	1	99	0.4	103	27	0.46	0.73
		59	63	0.3	75			
64	L-F-Phe	1	305	0.5	463	121	2.3	0.93
		64	288	0.3	430			
66	L-Trp	1	90	0.8	190	49	1.1	1.13
		66	134	0.7	215			
71	N-BnGly	1	55	0.6	100	26	2.4	8.33
		71	701	0.3	833			
72	L-Phe-Gly-1	1	9	0.4	16	4	NA	NA
		72	NA	NA	BLQ			
74	L-Phe-Sar-1	1	794	1	1533	399	4.0	0.001
		74	3	0.3	1			
78	D-Phe-Gly-1	1	51	0.5	307	80	3.7	3.66
		78	300	0.4	1124			
81	N-Me-L-Phe-Sar-1	1	160	0.3	92	24	NA	NA
		81	NA	NA	BLQ			
82	N,N-dimethyl-L-Phe-Sar-1	1	285	0.5	359	93	3.6	2.80
		82	432	0.4	1033			

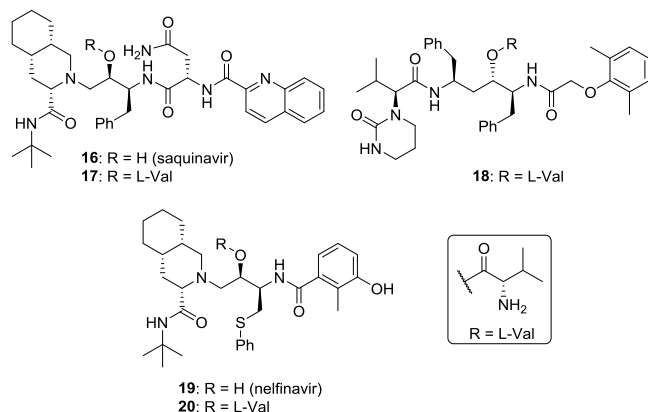
^aValues shown are mean \pm SD ($n = 3$). Parent drug **1** was dosed at 3 mg/kg, while the prodrugs were dosed at an equivalent dose of 3 mg/kg of **1**. NA = not available, BLQ = below limit of quantification. The formulation used for these experiments was 10% v/v DMAc, 40% v/v PEG-400, 50% v/v of 30% w/v HP β CD in pH 4.0 citrate buffer (50 mM). ^bThe oral bioavailability of **1** = 20%. ^cAUC of the intermediate is also included in the AUC of the prodrug.

prodrugs **17**, **18**, and **20** of PIs like **7**, saquinavir (**16**), and nelfinavir (**19**), guided the initial investigation of prodrugs of **1** which focused on valine derivatives.^{41–44} The oral bioavailability of **12** was significantly improved by taking advantage of

the L-Val ester prodrug **13** which is recognized as a substrate by PepT1 and unmasked in vivo by valacyclovirase, a serine hydrolase enzyme that cleaves an α -amino ester bond with high specificity.⁴⁵ Stereoisomeric Val amino acid and Val-Val



dipeptide prodrugs of **16** have been reported to reduce efflux ratio in Caco-2 cells and to improve metabolic stability in rat liver microsomes (RLM) relative to **16**.⁴² We have briefly described the L-Val amino acid prodrug of **1** in a previous publication in the context of designing a traceless acyl migration prodrug.¹⁶



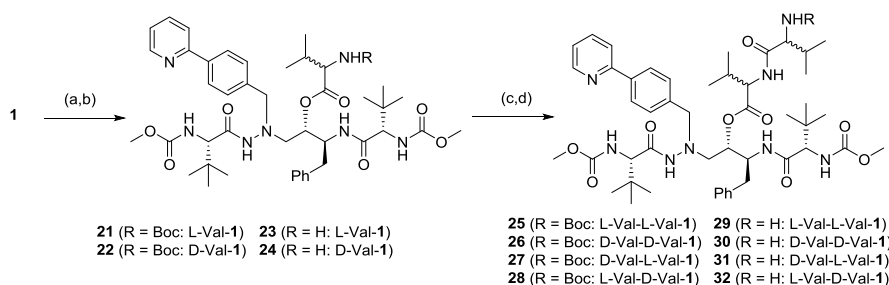
The diastereomeric Val amino acid prodrugs **23** and **24** derived from **1** were synthesized in two steps involving esterification of **1** with *N*-Boc-L-Val or *N*-Boc-D-Val using *N,N'*-dicyclohexylcarbodiimide (DCC) to afford **21** and **22**, respectively, followed by deprotection of the amine using 4 N HCl in dioxane to give **23** and **24**, which were isolated as their HCl salts (Scheme 2). The four stereoisomeric Val-Val dipeptide prodrugs **29**–**32** were synthetically derived from the corresponding amino acid prodrugs **23** and **24** by coupling with *N*-Boc-L-Val or *N*-Boc-D-Val using the HATU reagent with subsequent acid-mediated unmasking of the amino group (Scheme 2).

The Val-based amino acid and dipeptide prodrugs of **1** showed excellent chemical stability across the pH range of 1–6.5, with $t_{1/2}$ values of greater than 330 h, data that are summarized in Table 2. These compounds exhibited high aqueous solubility in the pH range of 1–6.5, with solubility decreasing with increasing pH. Importantly, these prodrugs

demonstrated at least 500-fold higher solubility at pH 6.5 than **1**, suggesting the potential to mitigate not only dissolution-limited absorption but also pH-dependent absorption. Although the isomeric prodrugs might be expected to show different physical and chemical properties because of their diastereomeric nature, no significant differences in solution stability or solubility parameters were observed.

With these data in hand, select Val-based compounds were progressed to oral PK studies in SD rats. Although the direct L-Val and other amino acid prodrugs of PIs like **7**, **16**, and **19** have been reported, these studies have mainly focused on in vitro characterization for determining chemical stability, aqueous solubility, permeability, active transport, and/or metabolic stability.^{18–20,23,41,44,46–48} Because PK data for most of these prodrugs are not readily available, it is difficult to assess their susceptibility to bioconversion in vivo and their capacity to improve the oral bioavailability of their respective parent PIs. In addition, there is an absence of a description of the effects of amino acid composition on the PK outcome that might have provided insights for the present study to guide the selection of amino acids. As is evident from the data compiled in Table 4, the amino acid-based prodrugs **23**, **24**, **29**, and **30** delivered lower plasma exposure of **1** than that observed following the direct administration of the parent drug. However, a significant systemic exposure of circulating prodrugs was observed and, in the case of the dipeptide-based prodrugs, varying levels of mono-amino acid ester intermediates were also noted. These in vivo PK studies facilitated three key conclusions: First, the direct Val amino acid and Val-Val dipeptide prodrugs were not susceptible to a substantial level of bioactivation, indicating that the crucial ester bond at the pharmacophoric 2° alcohol of **1** is recognized poorly by esterases and/or peptidases in the rat. Second, the observation of the formation of intermediate mono-amino acid esters in the case of dipeptide derivatives suggests a process of stepwise degradation of the dipeptide moieties to release amino acids, with subsequent degradation of these intermediates to release **1**. Third, as a result of the observation of a 10- to 14-fold higher relative total AUC (total AUC = AUC_{prodrug} + AUC_{intermediate} + AUC_{ATV}) of amino acid- and dipeptide-based prodrugs compared with that of **1**, it appears that these prodrugs significantly mitigated the barriers to oral bioavailability associated with **1**, including solubility-limited absorption, efflux, and, possibly, CYP-mediated metabolism. In terms of the influence of stereochemistry of the amino acid moieties, the L-Val prodrug **23** showed slightly better exposure

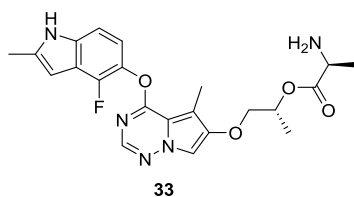
Scheme 2. Synthesis of Stereoisomeric Val-Based Ester **23** and **24** and Val-Val-Based Dipeptide Ester Prodrugs **29**–**32** of **1**⁴



⁴Reagents and conditions: (a) *N*-Boc-L-Val for **21** or *N*-Boc-D-Val, DCC, 4-dimethylaminopyridine (DMAP), CH₂Cl₂, RT, 14 h; yields: **21** = 41%; **22** = 23%; (b) 4 N HCl in dioxane, CH₂Cl₂, 0 °C to RT, 1 h; yields: **23** = 85%; **24** = 88%. (c) *N*-Boc-L-Val for **25** and **27** or *N*-Boc-D-Val for **26** and **28**, HATU, DIPEA, CH₂Cl₂, RT, 14 h; yields: **25** = 45%, **26** = 42%, **27** = 58%, **28** = 64%; (d) 4 N HCl in dioxane, 0 °C to RT, 1 h; yields: **29** = 76%, **30** = 80%, **31** = 85%, **32** = 81%.

than the D-Val prodrug **24**. In the case of the dipeptide-based prodrugs, the D-Val-D-Val prodrug **30** showed slightly higher exposure than the corresponding L-Val-L-Val prodrug **29**. In addition, the D-Val amino acid ester intermediate **24** from the D-Val-D-Val prodrug **30** was observed in circulation at significantly higher levels than the L-Val amino acid ester **23** derived from the L-Val-L-Val dipeptide **29**, indicating an effect of stereochemical recognition on the rate of enzymatic activation of the peptidic bond.

With the limitations posed by the L-Val-based prodrugs, an expansion of the scope of the amino acid promoiety was explored in an attempt to further develop SARs associated with the susceptibility to bioactivation. A small set of 5 different amino acid ester prodrugs (Gly and its *N*-methyl analogues, Ala, Leu, Met, and Phe) was considered. These can be divided into three categories: amino acids that lack an α -carbon substituent (Gly and its mono- and di-*N*-methyl analogues); amino acids that possess a smaller $C\alpha$ -substituent than that of L-Val (Ala); and amino acids that have a larger $C\alpha$ -substituent than L-Val (Leu, Met, and Phe). Of particular interest were amino acid promoieties like Gly and Ala with smaller $C\alpha$ -substituents than that of L-Val, based on the hypothesis that the corresponding prodrugs may be susceptible to a higher level of bioactivation compared with L-Val because of the reduced steric hindrance adjacent to the ester moiety. In support of this hypothesis, brivanib alaninate (BMS-582664, **33**) has been shown to undergo rapid and efficient enzyme-mediated hydrolysis, both in vitro and in vivo, to release the active drug.^{49,50}

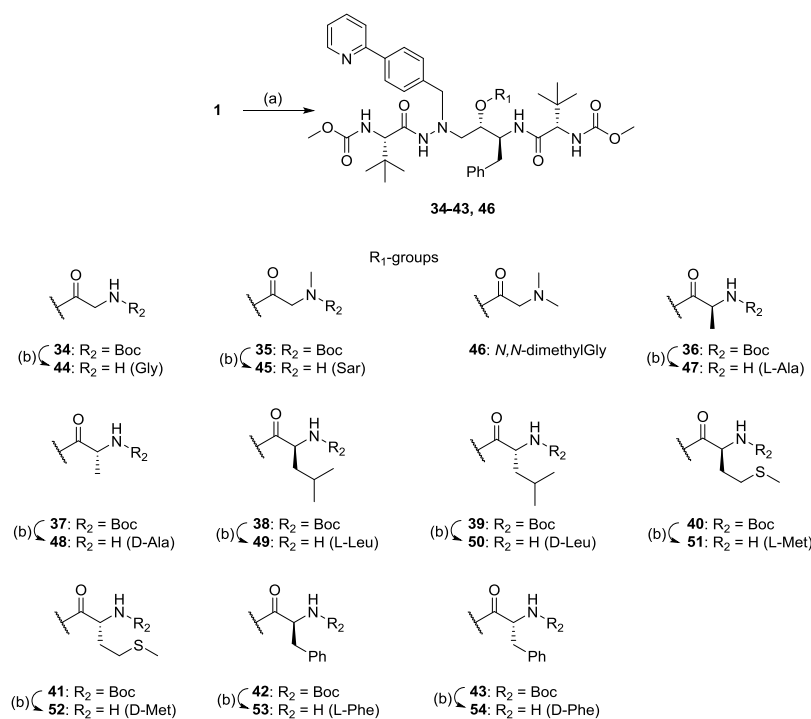


Prodrugs **44–54** were synthesized following the two-step procedure depicted in Scheme 3, and the data for these compounds are compiled in Table 2 (solubility and stability) and 4 (PK profiles). This set of prodrugs showed excellent stability ($t_{1/2}$ greater than 330 h) at pH = 1 and 4 but stabilities varied at pH = 6.5, with $t_{1/2}$ values ranging from 25 to 500 h (Table 2). With the exception of the Phe derivatives, these prodrugs displayed lower stability at pH 6.5 ($t_{1/2}$ = 25–188 h), when compared with the Val-based prodrugs. The solution stability at pH = 6.5 increased in the order of Gly \approx Ala < Leu < Met < Phe \approx Val, suggesting a trend of decreasing hydrolytic susceptibility with increasing steric crowding around the amino acid ester bond of **1**. Among the Gly-based prodrugs, the chemical stability increased in the order of Sar (**45**) < Gly (**44**) < *N,N*-dimethyl-Gly (**46**) at pH = 6.5, indicating that the introduction of one methyl group resulted in a slightly lower stability, but the introduction of two methyl groups resulted in \sim 4-fold improved stability when compared with the Gly-based prototype **44**. As was observed in the case of Val prodrugs, there were no significant differences in buffer stability and solubility between the diastereomeric prodrugs. All of these prodrugs showed very high solubility at pH = 1 and 4 (\geq 450 μ g/mL) but more variable solubility at pH = 6.5 (<1 to 930 μ g/mL). Amino acid prodrugs like **44–46** (Gly and its *N*-Me derivatives) and **47** and **48** (Ala), which had smaller $C\alpha$ -substituents than the L-Val derivative **23**, showed aqueous

solubility of greater than 360 μ g/mL at pH = 6.5, comparable to that of **23** (500 μ g/mL). In contrast, the Leu, Met, and Phe esters **50–54** displayed significantly reduced buffer solubility, in the range of 1–45 μ g/mL at pH = 6.5, which can be attributed to the increased lipophilicity associated with the $C\alpha$ -substituents which are bulkier than that in **23**.

Select prodrugs were progressed into rat PK studies to compare the AUC profiles and prodrug-to-parent ratios with that of the L-Val prodrug **23**. The L-Phe derivative **53** showed significantly improved oral exposure of **1**, with a 50% higher plasma exposure (AUC_{last}) observed than that following direct dosing of **1** and a 14-fold higher plasma AUC of **1** than that following dosing of **23** (Table 4). The oral exposure of **53** was also two-fold higher than that of the solubility-enhancing POM prodrug **11**, suggesting potential advantages of amino acid-based prodrugs to overcome additional barriers to oral bioavailability. Prodrug **53** also exhibited a significantly reduced prodrug/parent ratio of 1.2 compared with the ratio of 113 observed with the L-Val prodrug **23**, suggesting that the L-Phe ester **53** was more readily recognized by proteolytic enzymes than **23**. In addition, **53** showed a nine-fold lower prodrug/parent ratio when compared with the D-Phe-based prodrug **54**, indicative of a more efficient proteolytic bioactivation of the natural L-Phe prodrug **53** than the unnatural D-Phe congener **54** (Table 4). All of the other prodrugs in this set produced a lower exposure of **1** than that obtained following the direct administration of parent drug, although prodrugs **44** (Gly), **47** (L-Ala), and **49** (L-Leu) showed at least a two-fold better exposure of **1** when compared with **23**. Of the three Gly-based prodrugs examined, **44** exhibited the highest exposure of **1**, with the relative AUC values increasing in the order of Sar (**45**, 12%) < *N,N*-dimethylGly (**46**, 22%) < Gly (**44**, 58%). Of the two pairs of stereoisomeric prodrugs that were evaluated, **47** and **53** showed at least three-fold higher exposure than their corresponding D-amino acid homologues **48** and **54**, respectively. In terms of relative total AUC (combined exposures of **1** + prodrug), the D-Phe derivative **54** exhibited the highest exposure (4.5-fold) followed by the *N,N*-dimethyl glycine ester **46** (4.1-fold) and the L-Phe derivative **53** (3.3-fold). However, the total AUC values associated with these prodrugs were still lower than that of the Val-based prodrugs (10–12-fold higher AUC compared with the AUC obtained following direct dosing of **1**).

Encouraged by the improved plasma exposure of **1** following dosing of the L-Phe derivative **53** at a dose of 3 mg/kg, the PK performance of the prodrug in a dose-escalation study was investigated (Table 5). At doses equivalent to 6 mg/kg and 30 mg/kg of **1**, prodrug **53** exhibited approximately 2-fold and 34-fold higher exposure of the parent drug compared with the exposure obtained following administration of **53** at a dose equivalent to 3 mg/kg of **1**. Dosing of **53** afforded 4-fold and 65-fold higher total exposure of **1** + prodrug at 6 and 30 mg/kg equivalent doses, respectively, when compared with the exposure obtained following the direct dosing of **1** at a dose of 3 mg/kg. While the systemic exposure of **1** after dosing at the equivalent of 6 mg/kg of **53** was dose-proportional, the oral exposure at 30 mg/kg dose was more than dose-proportional. Prodrug **53** exhibited a decreasing prodrug-to-parent ratio with increasing dose, indicating a higher level of bioactivation as the dose was escalated. At 3- and 6-mg/kg-equivalent doses, the trough concentration of **1** from dosing with **53** measured at 24 h post-dose was below the limit of

Scheme 3. Synthesis of Amino Acid Prodrugs of **1** in Which Smaller or Larger Amino Acid Residues than That of *L*-Val Are Explored^a

^aReagents and conditions. (a) *N*-Boc-amino acid except in the case of **46**, for which dimethylglycine was used, DCC, DMAP, CH₂Cl₂, RT, 14–16 h; yields: **34** = 76%, **35** = 64%, **46** = 57%, **36** = 64%, **37** = 60%, **38** = 37%, **39** = 42%, **40** = 49%, **41** = 45%, **42** = 74%, **43** = 71%; (b) for all *N*-Boc derivatives: 4 N HCl in dioxane, 0 °C to RT, 1–2 h.; yield: **44** = 89%, **45** = 19%, **47** = 98%, **48** = 99%, **49** = 76%, **50** = 80%, **51** = 94%, **52** = 94%, **53** = 85%, **54** = 95%.

Table 5. Dose-Escalation PK Data for the *L*-Phe Prodrug **53** at Doses Equivalent to **6** and **30** mg/kg of **1**^a

compound	dose ^b	analyte	C _{max} (nM)	t _{max} (h)	AUC _{last} (nM h)	C _{trough} at 24 h (nM)	relative ATV exposure from the prodrug (%)	relative total AUC (prodrug + parent) (fold change)	prodrug/parent ratio
1	3	1	266	0.5	384	0.25			
53	3	1	456	0.5	573	BLQ	149	3.3	1.2
		53	474	0.5	686				
6	6	1	550	0.5	913	BLQ	238	4.1	0.7
		53	874	0.2	680				
30	30	1	4720	0.8	19670	1.0	5122	65.3	0.3
		53	2314	0.2	5409				

^aValues shown are mean ± SD (*n* = 3). NA = not available, BLQ = below limit of quantification. The formulation used for these experiments was 10% v/v DMAc, 40% v/v PEG-400, 50% v/v of 30% w/v HPβCD in pH 4.0 citrate buffer (50 mM). ^bDose for **53** = equivalent dose of the parent.

quantification (BLQ), although **1** was detectable at a concentration of 1 nM following a 30 mg/kg-equivalent dose. While the parent drug **1** furnished a C_{min} of 0.25 nM at 3 mg/kg dose, the absence of measurable trough levels of **1** from **53** indicates the inferiority of this prodrug compared with the parent on this important PK parameter. One of the important criteria for the selection of a prodrug candidate is that it should exhibit a C_{trough} of **1** that is comparable to or improved over the C_{trough} obtained following direct administration of the parent.

Having identified **53** as the lead prodrug from this cohort, a set of profiling studies was undertaken that were designed to understand pharmaceutical aspects, mechanism of bioactivation, and key safety aspects associated with hepatic uridine diphosphate glucuronosyltransferase 1A1 (UGT1A1) inhibition. The aqueous solubility of **53** was evaluated in additional buffers where it differentiated from **1** in the pH range of 3–6.5, with 27- to 4100-fold improved solubility (Table 6). The

Table 6. Extended aqueous Solubility Profiling of the *L*-Phe Prodrug **53**^a

medium	aqueous solubility (mg/mL)		fold improved solubility of 53 vs 1
	53	1	
pH 1 buffer	>1.5	1.69	
pH 3 buffer	>3.2	0.028	114
pH 4 citrate buffer	>1.1	<0.001	1100
pH 4 acetate buffer	>4.1	<0.001	4100
pH 5 buffer	1.3	<0.001	1300
pH 6.5 buffer	0.027	<0.001	27
pH 7.4 buffer	0.001	<0.001	
FaSSiF	0.13	ND	
FeSSiF	>0.5	ND	

^aND = not determined.

dissolution and solubility profile of **53** in biorelevant simulated small intestinal media which more effectively mimic the physiological conditions of the small intestine than simple buffers was also evaluated because this can be a useful approach to predicting the performance of a formulation in vivo while assessing the potential for a food effect as part of the modeling of the drug absorption process (Table 6).⁵¹ In both fasted-state simulated intestinal fluids (FaSSIF) and fed-state simulated intestinal fluids (FeSSIF), which contain natural solubilizers like bile salts and lecithin in amounts similar to natural intestinal fluids, **53** displayed an acceptable solubility of 0.13–0.5 g/mL.

Prodrug **53** was found to be stable following incubation with simulated gastric fluid (SGF) containing pepsin, an endopeptidase that is one of the main digestive enzymes produced in the stomach (see Figure 3, the Supporting Information). Pepsin is known to specifically cleave peptides at amino acid residues L-Phe, L-Met, L-Leu, and L-Trp when adjacent to a hydrophobic amino acid and the high gastric stability of **53** may be linked to the lack of susceptibility of the prodrug ester bond to pepsin.⁵² However, **53** was found to be unstable in simulated intestinal fluid (SIF) containing pancreatin, with the formation of **1** as the only product observed following incubation. This suggests that pancreatin, which is a mixture of several digestive enzymes (including lipase, amylase, and protease) produced in the pancreas by exocrine cells and is mainly responsible for the intestinal breakdown of peptides, might have contributed to the cleavage of the ester prodrug moiety of **53** in SIF.⁵² These data also suggest the potential for significant metabolic activation in the intestine and are consistent with the high intestinal turnover observed in rat closed loop studies (vide infra).

To further understand the mechanistic aspects of bioconversion, the metabolic susceptibility of **53** was evaluated in four different experiments as follows: (a) incubation in rat hepatocytes in the absence of additives; (b) incubation in rat hepatocytes in the presence of the esterase inhibitor phenylmethylsulfonyl fluoride (PMSF); (c) incubation in rat hepatocytes in the presence of the CYP 450 inhibitor 1-aminobenzotriazole (ABT); and (d) incubation in rat hepatocytes in the presence of both PMSF and ABT. PMSF is known to inhibit proteases (e.g., trypsin, chymotrypsin, thrombin, and papain) by reacting with the active site serine residue. As a non-isoform-specific and mechanism-based inhibitor of CYP enzymes, ABT is widely used to determine the relative contribution of oxidative metabolism in preclinical studies.⁵³ Significant turnover of **53** was observed in control rat hepatocytes, with a half-life of 42 min (Table 7 and Figure 4, the Supporting Information). However, this half-life was longer than that of the parent (27 min), indicating a modest reduction in the metabolic clearance of the prodrug compared with the

parent drug (Table 7). In the presence of PMSF, the rate of metabolic depletion of the prodrug in rat hepatocytes was reduced further, with the $t_{1/2}$ value extending to 77 min. Following co-incubation of **53** in rat hepatocytes in the presence of ABT, the half-life exceeded the assay time of 120 min, indicating that the metabolism of **53** was almost completely halted under these assay conditions. The combined presence of both PMSF and ABT in rat hepatocytes further improved the metabolic stability of **53** (Table 7 and Figure 4a, the Supporting Information). The significant enhancement in the elimination half-life of **53** in the presence of ABT compared with that in rat hepatocytes alone suggests that the prodrug is subject to direct metabolic clearance mediated by CYP 450 enzymes. In addition, the impact of esterase inhibition on the elimination rate of **53** was significantly less than the impact of CYP inhibition, indicating that the CYP-mediated metabolism was substantially higher than esterase-mediated degradation.

The formation of **1** from **53** was also monitored when the prodrug was incubated in rat hepatocytes alone or in the presence of PMSF and/or ABT (Table 7 and Figure 4b, the Supporting Information). The generation of **1** from **53** was minimal in the presence of PMSF alone or with a mixture of PMSF and ABT in rat hepatocytes, results that suggest that PMSF inhibits the esterase-mediated cleavage of **53** to deliver **1**. In contrast, the abundance of **1** was maximal in the presence of ABT alone, with the amount of **1** observed in the presence of ABT reduced by more than 90% by the addition of PMSF. This observation indicates that suppression of unproductive metabolism of **53** and/or **1** by ABT in the absence of inhibition of esterase-mediated prodrug conversion led to the highest levels of **1** in rat hepatocytes. Combining these results, it can be concluded that the formation of **1** from **53** is predominantly mediated by esterase-dependent prodrug activation. Although the in vitro system demonstrates efficient cleavage of **53** in hepatocytes, conversion of **53** into **1** following IV dosing is lower when compared with PO dosing, suggesting the potential for a contribution from intestinal metabolism in prodrug activation. Assuming proteolytic ester cleavage of **53**, the prodrug is expected to release L-Phe as the byproduct in vivo, a ubiquitous natural amino acid that should not present a safety concern. However, regulation of the intake of L-Phe may be required in those individuals who express a genetic polymorphism in phenylalanine hydroxylase, an enzyme that metabolizes L-Phe to L-Tyr in the human body.⁵⁴

An assessment of the activation of **53** in the intestine using a closed loop rat intestinal model was conducted to understand the bioconversion of the prodrug prior to or during absorption. The in situ intestinal perfusion technique in rodents has been useful as a model to understand the mechanisms underlying intestinal drug absorption.⁵⁵ The introduction of the mesenteric vein cannulation, which allows for the determination of the appearance of compounds in the blood, is particularly useful for evaluating mechanistic aspects of the absorption of compounds and prodrugs undergoing intestinal metabolism. Following cassette dosing of **53** and the low permeability marker nadolol at a dose of 1 mg/kg to rats, the observed levels of **1** in the mesenteric vein plasma were about 50% of prodrug **53**, suggesting the occurrence of significant prodrug activation in rat intestine (Table 8 and Figure 5, the Supporting Information). The parent drug **1** was also observed to be produced in intestinal tissue (29% of the prodrug **53**) and intestinal contents (50% of **53**). In the case of nadolol, the

Table 7. In Vitro Metabolic Stability Profile of L-Phe Prodrug **53 in Rat Hepatocytes in the Absence or Presence of Esterase and/or CYP Inhibitors**

additive		degradation data	
PMSF	ABT	$t_{1/2}$ (min)	k_{obs} (min ⁻¹)
no	no	42	0.0164
yes	no	77	0.0009
no	yes	>120	0.0042
yes	yes	>120	0.0014

Table 8. Assessment of the Activation of 53 in the Intestine Using a Closed Loop Intestinal Model Conducted in the Rat^a

compound	recovered percentage of dose of prodrug administered			
	mesenteric vein plasma (%)	intestinal homogenate (%)	intestinal content (%)	recovery (%)
53	2.8 ± 0.02	5.6 ± 1.0	32 ± 3.8	41 ± 2.8
1	1.4 ± 0.2	1.6 ± 0.2	16.1 ± 1.9	19 ± 1.9
total	4.2	7.2	48	60
nadolol	1.3 ± 0.1	14 ± 1.0	45 ± 11	61 ± 10

^aCassette dosing of the prodrug 53 and nadolol at 1 mg/kg each; formulation vehicle = PEG 400/TPGS/pH 6.5 buffer (25:5:70); values shown are mean ± SD (*n* = 3).

amount absorbed into plasma was 1.3% and recovery was 61%. Overall, these data imply that in the rat, the intestine plays a significant role in the conversion of 53 to 1. While the ratio of prodrug 53 to parent 1 in plasma in the closed loop study was ~2:1 (32% of parent 1; 68% of 53) following a dose of 1 mg/kg, the relative plasma concentration of parent and prodrug in the conventional oral PK study was 1:1. In addition, the prodrug was found to be highly stable in rat blood in vitro, with a *t*_{1/2} value of greater than 120 min. Taking all of these factors into account, it can be suggested that the initial formation of 1 from 53 occurs in the intestine with further conversion occurring in the liver.

Patients who are treated with 1 can experience asymptomatic hyperbilirubinemia because 1 is known to inhibit UGT1A1, thereby interfering with the glucuronidation and elimination of bilirubin.^{56,57} The potential for inhibition of bilirubin glucuronidation by the L-Phe prodrug 53 was assessed in vitro following separate incubations with recombinant human and cynomolgus monkey UGT1A1 protein as well as human and RLMs. For the purpose of comparison under the same experimental conditions, UGT1A1 IC₅₀ data for 1 were also generated. As is evident from the data compiled in Table 9, prodrug 53 showed four- to nine-fold lower inhibition of

Table 9. Cross-Species UGT1A1 Inhibition Profile of 1 and the L-Phe-Based Prodrug 53

substrate	enzyme preparation	prodrug 53 IC ₅₀ (μM)	parent 1 IC ₅₀ (μM)	prodrug selectivity
bilirubin	human rUGT1A1	2.8	0.3	9.3
	cynomolgus monkey rUGT1A1	11.9	0.7	17.0
β-estradiol	rat rUGT1A1	12.6	4.2	3.0
	HLM	2.5	0.6	4.2
	RLM	19.5	3.4	5.7

UGT1A1 when compared with 1. In a human rUGT1A1 study, 53 exhibited ~9-fold lower inhibitory potency than 1 while in human liver microsomes (HLM), 53 demonstrated ~4-fold reduced potential for inhibition of glucuronidation than 1. The lower activity of prodrug 53 toward UGT1A1 inhibition compared with the parent was consistent in other species including the cynomolgus monkey (rUGT1A1) and rat (rUGT1A1 and RLM). However, the potential advantage of the reduced inhibitory effect on UGT1A1 needs to be carefully considered in the context of the C_{max} and free drug

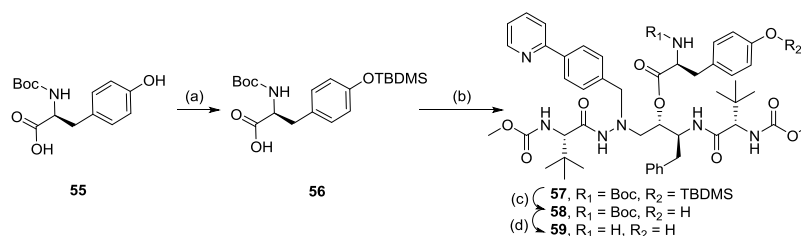
concentrations of both the released parent 1 and 53 at the efficacious dose.

With these data in hand, the design considerations for further optimization of the profile of 53 focused on analogues that encompassed both relatively simple structural variations that included substitution on the phenyl ring of the promoiety and more complex variations in which the phenyl ring was replaced with a heteroaryl variant or the benzyl group was translocated from the α-carbon to the amino group. This phase of the study explored four different amino acid ester prodrugs, all bearing an aryl group, with the objective of further optimizing the prodrug performance as a means of improving exposure and, particularly, the trough concentration of 1 measured at 24 h postdose. The L-Tyr prodrug 59 was explored in an effort to understand whether a potential metabolite of 53 would offer differentiation in terms of rate of in vivo conversion to the parent. This is in line with the results of biotransformation studies conducted with 53 which suggested that hydroxylation of L-Phe promoiety was one of the metabolic pathways. Compound 59 was synthesized in 4 steps as depicted in Scheme 4. The phenolic hydroxyl of N-Boc-L-Tyr 55 was protected as its silyl ether by treatment with TBDMS-Cl to afford 56 which was converted to the ester 57 by DCC-mediated coupling with 1. Treatment of 57 with TBAF removed the silicon protecting group and afforded intermediate 58 which was subjected to amine deprotection on treatment with 4 N HCl in dioxane to afford the L-Tyr derivative 59.

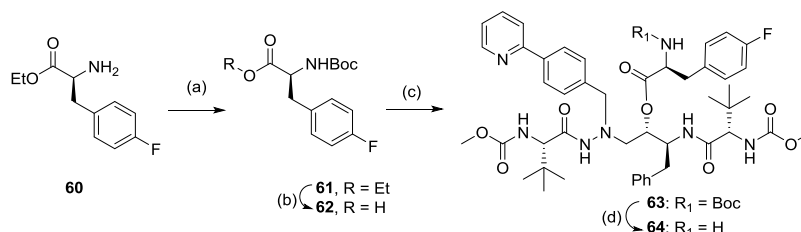
The effect introducing a fluorine substituent to the phenyl ring of the L-Phe element of 53 was examined because the strategic incorporation of this element can productively modulate several aspects of molecular properties that encompass molecular conformation, pK_a, lipophilicity, intrinsic potency, permeability, metabolic pathways, and PK properties.^{58–61} Thus, the 4-fluoro-Phe derivative 64 was prepared because this substitution may influence oxidative metabolism of 53 should that occur in vivo. Prodrug 64 was synthesized in four steps, as delineated in Scheme 5. The readily available amino ester intermediate 60 was protected as its Boc derivative 61, which in turn was subjected to hydrolysis using LiOH to afford the N-Boc amino acid 62. DCC-mediated coupling of 62 with 1 afforded 63 which was converted to the final compound 64 following acid-aided removal of the Boc group.

The L-Trp prodrug 66 was prepared from 1 following the two-step procedure captured in Scheme 6 while the N-benzylglycine (N-BnGly) prodrug 71 was given consideration as part of the effort to understand the potential impact of migrating the Cα-benzyl group from carbon to nitrogen on PK properties. This prodrug was synthesized in four steps from commercially available N-benzylglycine ethyl ester, as depicted in Scheme 6.

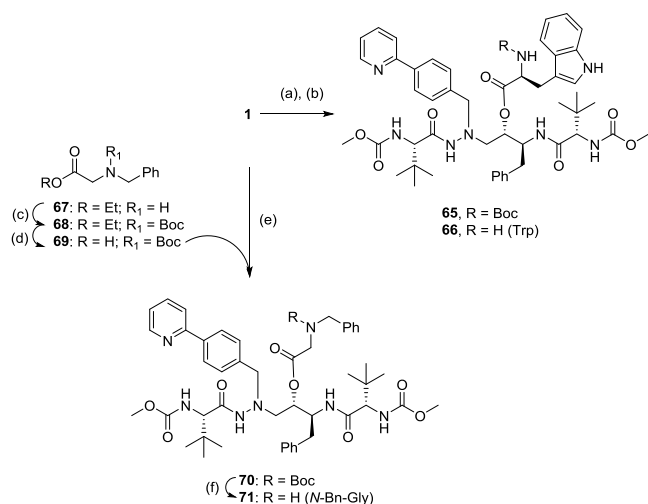
Compounds 59, 64, 66, and 71 exhibited acceptable stability across the pH range, although these prodrugs showed lower stability than 53 at pH = 6.5 (Table 2). However, these prodrugs showed improved stability compared with the Gly, Ala, Leu, and Met prodrugs 44, and 47–52, suggesting that the presence of an aromatic group in the amino acid residue contributes to reduced hydrolytic susceptibility at pH = 6.5. While 59, 64, 66, and 71 showed excellent solubility of at least 700 μg/mL at pH = 1 and 4, these prodrugs showed significantly reduced solubility of less than 10 μg/mL at pH = 6.5, attributable to the negative impact of the presence of a hydrophobic aryl group.⁶² This series of prodrugs exhibited

Scheme 4. Synthesis of the L-Tyrosine-Based Amino Acid Ester Prodrug 59^a

^aReagents and conditions. (a) TBDMS-Cl, imidazole, DMF, RT, 16 h, 62%; (b) **1**, DCC, DMAP, CH₂Cl₂, RT, 16 h, 68%; (c) TBAF, THF, 0 °C, 1 h, 72%; (d) 4 N HCl in dioxane, 0 °C to RT, 1 h, 84%.

Scheme 5. Synthesis of 4-Fluorophenylalanine Amino Acid Ester Prodrug 64^a

^aReagents and conditions. (a) (Boc)₂O, Et₃N, CH₂Cl₂, RT, 2 h, 95%; (b) LiOH, THF, H₂O, 0 °C, 2 h, 93%; (c) **1**, **62**, DCC, DMAP, CH₂Cl₂, RT, 16 h, 58%; (d) 4 N HCl in dioxane, 0 °C to RT, 1 h, 74%.

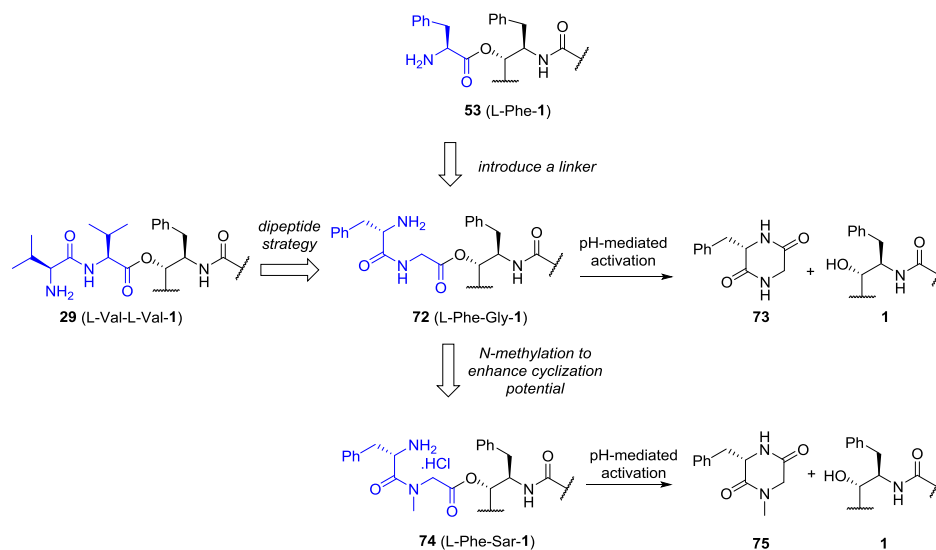
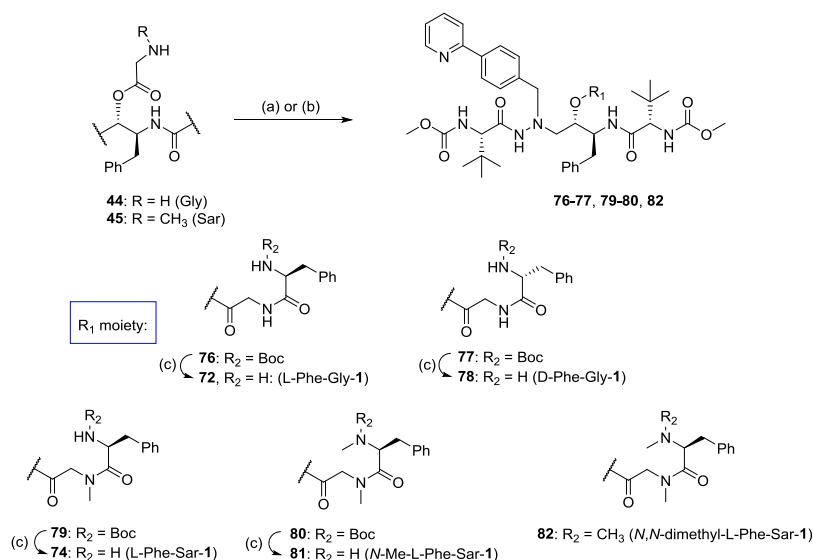
Scheme 6. Synthesis of L-Trp Amino Acid Ester Prodrug 66 and N-Benzylglycine Amino Acid Ester Prodrug 71^a

^aReagents and conditions. (a) *N*-Boc-Trp, DCC, DMAP, CH₂Cl₂, RT, 14 h, 52%; (b) 4 N HCl in dioxane, 0 °C to RT, 1 h, 68%. (c) (Boc)₂O, Et₃N, CH₂Cl₂, 0 °C to RT, 12 h, 92%; (d) LiOH, THF, H₂O, 0 °C, 2 h, 95%; (e) **69**, DCC, DMAP, CH₂Cl₂, RT, 16 h, 89%; (f) 4 N HCl in dioxane, 0 °C, 1 h, 95%.

plasma exposure of the parent that increased in the order **71** < **59** < **66** < **64** following oral administration to rats (Table 4). Prodrug **64** demonstrated a higher plasma AUC of **1** than that of the direct administration of the parent drug but the trough concentration of **1** from **64** was BLQ. The introduction of a 4-fluoro or 4-hydroxy substituent on the phenyl ring of **53** did not result in an improved exposure of **1**. Considering the total AUC of parent and prodrug, the *L*-F-Phe (**64**) and *N*-Bn-Gly (**71**) promoieties were found to be better than the promoieties *L*-Tyr (**59**) and *L*-Trp (**66**). While **64** and **71** provided a similar total AUC, **64** was found to undergo ~8-fold higher

conversion in vivo resulting in an improved AUC profile of **1** from **64**. Unfortunately, none of these prodrugs offered an advantage in terms of higher parent exposure over the lead prodrug **53**.

While **53** and **64** offered the benefit of improving the oral exposure of the parent, scope existed to further improve the oral bioavailability of **1** from these prodrugs and importantly demonstrate measurable levels of **1** at 24 h postdose that is critical for the systemic suppression of viral load. In this direction, the installation of a linker between **1** and the *L*-Phe moiety that was simpler than the *L*-Val elements studied earlier was explored in an effort to improve the efficiency of release of parent from the prodrug (Scheme 7). This design concept was inspired by published observations that dipeptide ester prodrugs can undergo intramolecular cyclization at physiological pH in which the terminal amine the dipeptide moiety attacks the ester carbonyl group, leading to the release of the parent drug along with the formation of a diketopiperazine byproduct.^{63–65} This chemo-activatable prodrug strategy was considered to offer the potential to address the bioactivation challenges that were encountered with the direct amino acid ester prodrugs discussed earlier. As a precedent, neladenoson bis-alanate, a clinical prodrug candidate of the partial adenosine A1 receptor agonist neladenoson, has recently been shown to significantly improve the oral bioavailability of the parent compound without the presence of circulating prodrug.⁶⁶ The stability pattern of the Val-Val dipeptides gave some insight into the design of the requisite linker. For example, the Val-Val dipeptide **29** displayed very high aqueous stability of *t*_{1/2} of more than 500 h at pH = 6.5, indicating that this prodrug is not able to efficiently engage in an intramolecular cyclization to generate the parent **1** under the conditions of elevated pH. This can be attributed to the high steric crowding around the ester bond of **29** because of the presence of the isopropyl element adjacent to the Val ester. In the case of dipeptide prodrugs of **12**, it has been shown that the rate of decomposition is significantly

Scheme 7. Linker-Enabled Chemo-Activatable Prodrug Design To Improve the Bioactivation of Prodrug 53 with the Prodrug Moieties Depicted in Blue

Scheme 8. Synthesis of L-Phe-Gly-1 (72), D-Phe-Gly-1 (78), L-Phe-Sar-1 (74), and the N-Me and N,N-Dimethyl Homologues 81 and 82 as Potential Dipeptide Ester-Based Prodrugs of 1^{4a}


^{4a}Reagents and conditions. (a) 44, *N*-Boc-L-Phe for 76 or *N*-Boc-D-Phe for 77, HATU, DIPEA, CH₂Cl₂, RT, 8 h; yields: 76 = 64%; 77 = 65%; (b) 45, *N*-Boc-L-Phe for 79, *N*-Boc-L-*N*-MePhe for 80, or L-*N,N*-dimethylPhe for 82, HATU, DIPEA, CH₂Cl₂, RT, 8 h; yields: 79 = 81%; 80 = 32%; 82 = 35%; (c) 4 N HCl in dioxane, 0 °C to RT, 1 h; yields: 72 = 72%; 78 = 93%; 74 = 98%; 81 = 87%.

decreased following the incorporation of sterically hindered amino acids into the dipeptide backbone and that the effect is more pronounced when a bulky β -branched amino acid like L-Val is present as the C-terminal residue that is directly attached to the drug.⁶⁷ It was postulated that Gly, which does not possess a C α -substituent, might be a good choice as a linker to promote a facile, self-immolative internal cyclization of 72 to generate the diketopiperazine 73 and parent 1, as depicted in Scheme 7. The Gly-Phe dipeptide prodrugs of various drugs that include acyclovir have previously been investigated as carrier prodrugs for delivering the active parents via a nonenzymatic process.⁶⁷ While the kinetics associated with self-immolation of prodrug 72 are inherent to the structure, it was hypothesized that the introduction of a substituent on the Phe-Gly amide NH would provide a means of modulating the

rate of ring closure, allowing a measure of control over drug release. Thus, the amide conformer topology would be influenced by N-methylation which would assist in bringing the terminal amine and ester carbonyl group in close proximity, thereby enhancing the propensity for cyclization.⁶⁵ Taking all of these factors into consideration, Gly and Sar were chosen as the amino acid linkers, leading to the design of L-Phe-Gly-1 (72) and L-Phe-Sar-1 (74) as potential prodrugs. On the basis of the design principle, these prodrugs would be expected to be stable in the stomach as the hydrochloride salt but hypothesized to convert to a free base in the intestine or during or after absorption, triggering a facile intramolecular cyclization to liberate the parent 1 and the diketopiperazine byproduct 73 or 75.

A set of 5 prodrugs was prepared by the routes depicted in Scheme 8 to develop SARs around solution stability, aqueous solubility, the rate of cyclization, and the potential for in vivo delivery, as measured by the exposure of **1** and prodrugs in plasma following oral administration. While prodrugs **72** and **78** were prepared from **44** in two steps, the remaining prodrugs **74**, **81**, and **82** were prepared from the readily available Sar prodrug **45** in two steps. Along with **72** and **74**, the synthesis of the three additional prodrugs **78**, **81**, and **82** was undertaken with the primary objective of broadening the SARs associated with these cyclization-activated prodrugs. The D-Phe-Sar-1 prodrug **78** was explored to understand whether the stereochemical switch in the promoiety would differentiate this diastereomer from **72** in terms of cyclization kinetics and oral exposure profile. Prodrug **81** was designed to understand the impact of N-methylation of the nucleophilic amine on modulating conversion kinetics of **74** and on plasma exposure of **1**, whereas the *N,N*-dimethyl-L-Phe-Sar-1 prodrug **82** was evaluated specifically as a means of gaining insight into the behavior of a prodrug incapable of undergoing cyclization-based self-immolation at physiological pH due to blockade of the amino terminus. Contrary to the possibility of chemical-mediated activation mechanism of **72**, **74**, **78**, and **81**, conversion of prodrug **82** would be expected to proceed by either an enzyme-mediated cleavage or by a general base-catalyzed process to deliver the parent in vivo.

While the L-Phe (**53**) and D-Phe (**54**) derivatives exhibited high aqueous stability across the pH range of 1–6.5, the introduction of a Gly linker, as in the case of **72** (L-Phe-Sar-1) and **78** (D-Phe-Sar-1), resulted in more than five-fold reduced stability at pH 6.5, with no impact on the high chemical stability observed at pH values of ≤ 4 (Table 2). Prodrug **78**, which incorporates an unnatural D-Phe in the promoiety ($t_{1/2} = 89$ h), revealed slightly higher stability than the diastereomeric prodrug **72** with a natural L-Phe in the promoiety ($t_{1/2} = 74$ h). The reduced stability of the dipeptide prodrugs at pH 6.5 can be attributed to the tendency to undergo deprotonation at higher pH values which will facilitate intramolecular cyclization to release **1**. Self-immolative activation was further accelerated in the L-Phe-Sar prodrug **74** where the *N*-methyl group would lead to significant population of the *cis*-amide topology which is primed for cyclization to the diketopiperazine to release **1**. At a pH value of 6.5, L-Phe-Sar-1 (**74**) cyclized completely within 60 min, with a $t_{1/2}$ estimated to be on the order of 5 min. The intramolecular cyclization of **74** in pH 6.5 buffer was confirmed with the observation of formation of the corresponding diketopiperazine **75** by LCMS as the only byproduct (Scheme 7 and Table 10). Monomethylation of the nucleophilic terminal amine of **74** gave **81** which offered no differentiation in solution stability at pH = 6.5; however, the dimethyl homologue **82** was considerably more stable at pH values of ≥ 4 than **74**, consistent with the inability of this

prodrug to undergo facile intramolecular chemo-activated cyclization. The facility with which the L-Phe-Gly prodrug **72** cyclizes to release **1** contrasts with the relative stability of the L-Val-L-Val derivative **29**, indicating that the absence of the α -alkyl moiety enables intramolecular cyclization through population of a *cis*-amide conformation favorable for cyclization. While prodrugs **72** and **78** showed excellent solubility of at least 2000 $\mu\text{g/mL}$ at pH values of 1 and 4, these prodrugs demonstrated acceptable solubility of more than 200 $\mu\text{g/mL}$ at pH = 6.5, representing a more than 200-fold improvement in solubility compared with **1**. The installation of the Gly linker in prodrugs **72** and **78** was found to offer more than 20-fold and 200-fold increased solubility, respectively, compared with the monoester counterparts **53** and **54** that lack the linker. Prodrugs **74** and **81** demonstrated excellent aqueous solubility of more than 1000 $\mu\text{g/mL}$ at pH = 1, but the solubility could not be determined at pH = 4 and 6.5 because of the limited chemical stability under these conditions. However, the enhanced stability of **82** allowed determination of the solubility across the pH range with this prodrug, demonstrating solubility of greater than 1200 $\mu\text{g/mL}$ at pH 1–4 although the solubility was a more modest 20 $\mu\text{g/mL}$ at pH = 6.5.

Following oral administration of **72**, **74**, **78**, **81**, and **82** at a 3 mg/kg-equivalent dose of **1**, these prodrugs were found to deliver the parent in vivo, with the measured AUC values of **1** increasing in the order of $72 < 81 < 78 < 82 < 74$, results that are compiled in Table 4. Prodrug **74** demonstrated the highest exposure of **1**, with a relative oral AUC of $\sim 400\%$ compared with that of **1**, indicating a superior performance compared with all of the other prodrugs that have been investigated as part of this study. Importantly, **74** delivered an eight-fold higher C_{trough} concentration of **1** in the rat measured at 24 h postdose compared with administration of **1** in contrast with the earlier prodrugs, none of which furnished a measurable C_{trough} level of **1**. The relative oral bioavailability of **1** from **74** was four-fold higher (80%) compared with that of **1** following direct administration (20%). The prodrug/parent ratio measured for **82** was 2800-fold higher than that of **74**. This indicated that the bioconversion of **82**, which was mainly designed to undergo enzymatic hydrolysis, was a slow process, reflecting the challenges associated with prodrug activation mediated by proteases. However, the PK profile of **82** suggests that this prodrug may be suitable for a sustained release of the parent. The D-Phe-Gly-1 prodrug **78** afforded 20% higher oral exposure than the stereoisomeric L-Phe-Gly-1 prodrug **72** while the introduction of methyl group on the *N*-terminal amino group of **74** was found to be less favorable, with the observation of 17-fold reduced systemic exposure of parent from **81**.

Encouraged by the superior plasma exposure and C_{trough} value of **1** released from the L-Phe-Sar prodrug **74** at an equivalent dose of 3 mg/kg, the PK performance of the prodrug in a dose-escalation study was investigated (Table 11 and Figure 6, the Supporting Information). At a dose equivalent to 30 mg/kg of **1**, prodrug **74** exhibited 11-fold higher exposure of **1** compared with the exposure obtained following administration of **74** at a dose equivalent to 3 mg/kg of **1**. This indicates that the systemic exposure of **1** at a 30 mg/kg-equivalent dose was dose-proportional. Prodrug **74** also delivered a 16-fold higher C_{trough} level of **1** at the 30 mg/kg-equivalent dose of **1** than that of the 3 mg/kg-equivalent dose. Systemic circulation of **74** was not observed, indicating a

Table 10. Rate of Formation of the Cyclic Byproduct **75 along with **1** Associated with the Degradation of Prodrug **74** at pH = 6.5 in Buffer^a**

time (min)	74	75 (%)	1 (%)
2	86.1%	3.8	10.0
30	2.0%	29.7	68.4
60	NA ^a	31.0	69.0

^aNA = data not available.

Table 11. PK Data for the Prodrug 74 Following Dose Escalation

dose (mg/kg)	analyte	C_{\max} (nM)	t_{\max} (h)	AUC_{last} (nM h)	C_{trough} (nM) at 24 h	relative AUC of 1 from the prodrug ^a (%)	prodrug/parent ratio
3	1	794	1	1533	1.9	399	0.001
	74	3	0.3	1	BLQ		
30	1	8756	1	16580	30.4	4318	NA
	74	BLQ	BLQ	BLQ	BLQ		

^aThe prodrug 74 was dosed at an equivalent dose of 3 mg/kg and 30 mg/kg of the parent. Values shown are mean \pm SD ($n = 3$). Abbreviations used: NA = not applicable or not available, BLQ = below limit of quantification.

Table 12. Evaluation of the Permeability of Select Amino acid Prodrugs across a Caco-2 Monolayer

compound	promoiety	clog D (pH 6.5) ^a	HBD/HBA count ^a	PSA ^a	Caco-2 P_{app} (nm/s)		efflux ratio	AUC (nM h)		total AUC _(prodrug+ATV) / AUC _{ATV}
					A–B	B–A		prodrug	1	
1		4.5	5/7	171	<15	203	>14		384	
23	L-Val	4.5	5/7	205	<15	122	>8.1	4731	42	12.4
46	<i>N,N</i> -dimethyl-Gly	4.5	4/8	181	<15	132	>8.8	1519	45.7	4.0
53	L-Phe	5.7	5/8	203	<15	131	>8.7	686	573	3.3
59	L-Tyr	5.4	6/9	223	<15	71	>4.7	75	103	0.46
64	4-F-L-Phe	5.8	5/8	203	<15	82	>5.5	430	463	2.3
71	BnGly	6.1	5/8	189	<15	96	>6.4	833	100	2.4

^aPhysical properties (clog D , HBD count, HBA count, and PSA) were calculated using ChemAxon Marvin Sketch software. ^bTargeted concentration is 2 μM . Transport medium: 4% HSA in HBSS; permeability values have been calculated based on prodrug appearance only. Negligible levels of 1 were observed at the end of the incubation.

robust reversal of the prodrug to 1 following dose escalation. The potential in vivo byproduct 75 was not monitored in these studies and although this compound has been reported in the literature, its toxicological profile remains to be understood.⁶⁸ The potential safety concerns associated with the prodrug 74 itself appear to be limited because of the absence of systemic circulation of the prodrug.

The parent drug 1 appears to be the substrate for several transporters which, in turn, contributes to reduced oral systemic bioavailability, intracellular concentration, and brain bioavailability. As a class, PIs are the substrates for the ATP-binding cassette family of drug efflux transporters including P-gp, multidrug resistant proteins (MRPs), and breast cancer resistance protein (BCRP) and also anionic and cationic transporters like organic anion transporting polypeptide (OATP) and organic cation transporter (OCT).^{9,69,70} These transporters are differentially expressed at the important sites of drug disposition, including the intestine, lymphocytes, liver, brain, and kidney and, hence, play a significant role in the disposition of PIs, influencing oral absorption, tissue distribution, and cellular accumulation. Amino acid prodrugs of PIs have previously been shown to enhance absorptive permeability by engaging an active transport system and reducing efflux.²³ The apparent bidirectional Caco-2 permeability coefficients for 1 and select prodrugs was determined in an effort to understand whether the prodrugs could evade efflux transporters. The Caco-2 permeability assay represents an important in vitro system with which to predict human intestinal permeability and the absorption of oral drugs. In the co-solvent Caco-2 assay, 1 showed low apical-to-basolateral and high basolateral-to-apical permeability (Table 12) with the secretory flux of 1 >14-fold higher than its absorptive flux. These results are consistent with the literature characterization, indicating that 1 is a substrate for efflux transporters.⁹ Surprisingly, none of the tested prodrugs showed improved apical-to-basolateral permeability compared with the parent, irrespective of whether the cLog D values of these prodrugs

were similar to or higher than that of 1 (Table 12). However, the prodrugs differentiated from 1 in that they showed reduced potential for transepithelial efflux, suggestive of lower affinity of the prodrugs for the efflux transporters when compared with 1 (Figure 7, the Supporting Information). Amongst the prodrugs, 46 showed the highest efflux potential despite having the lowest HBD count (4), whereas 59, which has the highest HBD count (6), exhibited the lowest efflux ratio, suggesting an absence of a correlation between efflux and HBD count. With the exception of the L-Tyr prodrug 59, all of the prodrugs evaluated showed a 3- to 12-fold improvement in total oral systemic exposure of prodrug and 1 in rats, when compared with the direct administration of 1. On the basis of the in vitro Caco-2 permeability data, it can be hypothesized that reduced efflux partly contributes to the in vivo observation of improved total AUC of prodrug + 1. This is supported by the observation of a 12-fold increase in the brain-to-plasma ratio ($C_{\text{brain}}/C_{\text{plasma}}$) following IV administration of 1 to mice treated with the P-gp inhibitor elacridor compared with vehicle-treated mice.⁶⁹ Surprisingly, the Tyr prodrug 59 did not significantly improve the total AUC of prodrug + 1, although it showed the lowest efflux potential out of the prodrugs tested. Unlike other prodrugs, the Tyr prodrug 59 possesses a phenolic functionality that has calculated a pK_a value of 9.5, indicating that ionization in the intestine as a limiter of oral absorption can be ruled out.

An analysis of the complete set of the solubility data over the pH range of 6.5–7.4, which is considered to be the most relevant for intestinal absorption, indicates that the phosphate prodrugs 2 and 11 exhibited superior solubility, with the direct phosphate ester 2 showing the highest solubility (Figure 8, the Supporting Information). The direct phosphate prodrug 2 exhibited two-fold higher solubility than the POM prodrug 11, indicating that the introduction of a methylene spacer contributes to slightly reduced aqueous solubility. Among the amino acid prodrugs, those compounds with no amino acid side chain elements 44 (Gly), 45 (Sar), and 46 (*N,N*-dimethyl-

Gly) or with smaller residues like Me (Ala derivatives 47 and 48) and iPr (Val derivatives 23 and 24) exhibited high solubility, with a more than >200-fold advantage compared with 1. Those prodrugs with either a more lipophilic side chain (Leu and Met derivatives 49–52) or an aryl group (Phe derivatives 53, 54, and 64, Trp derivative 66, Tyr 59 and the Bn-Gly derivative 71) showed significantly decreased solubility that was in the range of 1–45 $\mu\text{g}/\text{mL}$. The dipeptide ester prodrugs 29–32, 72, and 78 demonstrated consistent increases in solubility of at least 230 $\mu\text{g}/\text{mL}$ in spite of the presence of two isopropyl moieties or an aromatic group. The only exception was the dipeptide prodrug 82 bearing a 3° amine, which showed at least 10-fold reduced solubility that can be attributed to the lack of 1° or 2° amine group. Consistent with this, the tertiary amine-based prodrugs 46 and 82 exhibited ~2.5-fold and 32-fold lower solubility than their primary amine counterparts 44 and 72, respectively. Expansion of the mono-Val amino acid esters 23 and 24 to the Val-Val dipeptide esters 29–32 did not exert a significant impact on the aqueous solubility.

An analysis of the AUC of 1 released from the prodrugs indicated that Phe-based, direct amino acid prodrugs with (*S*)-stereochemistry or Phe-based, dipeptide promoieties with the exception of 72 and 81 showed AUC values of 1 in the range of 307–1533 nM h, a profile that is similar to or higher than the AUC obtained after direct administration of 1 (Figure 9, the Supporting Information). These results suggest that the *L*-Phe derivatives 53 and 64 are more readily recognized by hydrolytic enzymes than the other amino acid-based prodrugs, contributing to the release of a higher amount of 1 from these prodrug moieties. The remainder of the amino acid prodrugs without a α substituent (Gly and its derivatives 44–46) or with a α substituent (47 and 48 (Ala), 23 and 24 (Val), 51 and 52 (Met), 66 (Trp), and 49 and 50 (Leu)) showed a lower AUC exposure of 1 when compared with dosing of the parent drug. Of the three *L*- and *D*-stereoisomeric pairs of amino acid prodrugs 23/24, 47/48, and 53/54 prepared, the *L*-amino acid prodrugs released a 2- to 12-fold higher amount of 1 in vivo. However, this trend was reversed in the case of the *L*- and *D*-stereoisomeric pairs of dipeptide prodrugs 29/30 (Val-Val-1) and 72 and 78 (Phe-Sar-1).

An analysis of the total AUC comprising the sum of the AUC of 1 arising from the prodrug and AUC of the circulating prodrug was undertaken to better understand the overall performance of these prodrugs in mitigating the physiological barriers for oral drug delivery. The prodrugs examined furnished a 1.1- to 14-fold higher relative total AUC of 1 compared with the AUC that was obtained after oral dosing of 1, with the exception of 11, 45, 48, 51, 59, 72, and 81 (Figure 10, the Supporting Information). These data further revealed the superior performance of the Val-based amino acid derivatives 23 and 24 and the dipeptide prodrugs 29 and 30, which offer 10- to 14-fold higher total oral AUCs than when dosing 1 directly. This indicates that prodrugs with Val or Val-Val residues are the most effective at mitigating the barriers to oral bioavailability through a combination of enhanced solubility, reduced efflux and reduced metabolism. However, these prodrugs do not appear to offer advantages in improving the absorptive permeability, another barrier for bioavailability. The Phe-derived direct prodrugs 53, 54 and 64 and dipeptide prodrugs 74, 78, and 82 also displayed higher relative total AUC values of 1 with a 2- to 4-fold enhancement compared with administration of a parent drug. With respect to the

stereoisomeric pairs studied, there was no consistent trend with respect to the particular configuration of the amino acid moiety.

In the early stages of the program, the prodrugs of 1 were tested for HIV-1 protease inhibition and antiviral activity in a HIV-1 replicating virus assay hosted by MT2 cells (see Table 13 and Figure 11, the Supporting Information). Although compounds with prodrug elements attached to the pharmacophoric hydroxyl moiety would not be expected to inhibit HIV-1 protease in a biochemical assay, the prodrug may be subject to cleavage in cell-based antiviral assays. Although the initial prodrugs prepared were tested in both assays, there was not a significant correlation between the activity observed in the biochemical and cell-based assays because factors including the permeability of the compound and activation of the prodrug by cellular enzymes are expected to play a role in the expression of cellular antiviral activity. As a consequence, later prodrugs were profiled only in the cell-based assay. Control compound 1 exhibited potent inhibition in the enzymatic assay ($\text{IC}_{50} = 0.3$ nM) as well as in the cellular assay ($\text{EC}_{50} = 0.7$ nM). Those prodrugs tested in the HIV-1 protease assay expressed inhibition with IC_{50} values in the range of 4–1145 nM, with cellular EC_{50} values observed across the range of 0.9–1250 nM. Prodrugs 23, 24, 29, 30, 44, 46, and 48 displayed enzymatic and cellular inhibitory activities that represented a less than three-fold difference between IC_{50} and EC_{50} values. The other prodrugs 31, 32, 47, 53, and 54 showed a significant 19- to 42-fold difference between the IC_{50} and EC_{50} values. Prodrugs 47, 53, and 54 exhibited markedly higher HIV-1 inhibitory activity in the cell-based assay compared with the IC_{50} values. In general, *L*-amino acid-based prodrugs exhibited better cellular anti-HIV-1 activity than *D*-amino acid-based prodrugs (compare 23 and 24, 47 and 48, 49 and 50, 51 and 52 and 53 and 54 in Table 13, the Supporting Information), consistent with the hypothesis that the natural amino acid esters can undergo cellular activation more readily to release the parent than the unnatural counterparts. Another SAR pattern in HIV-1 inhibitory activity that was apparent was the markedly lower cellular activity of Val mono-amino acid esters and Val-Val dipeptide esters (EC_{50} values range from 84 to 1250 nM) than the other amino acid esters (EC_{50} values range from 0.7 to 17 nM), as evident from the data compiled graphically in Figure 10. Thus, those prodrugs which have no branching on the β -carbon of the amino acid showed higher antiviral activity than the Val prodrugs which possess β -branching. One of the possible reasons behind this observation is that the prodrugs that lack branching on the β -carbon of the amino acid moiety may be subject to a higher rate of enzymatic cleavage to release 1 which mediates the antiviral activity in cell culture. Additional studies are required to confirm if amino acid or dipeptide prodrugs are intrinsically active or if the activity is derived from the parent after hydrolytic conversion of the prodrugs to 1 in HIV infected cells.

CONCLUSION

A survey of the in vitro and in vivo performance of a series of phosphate and amino acid-based prodrugs of the HIV-1 PI 1 identified the *L*-Phe-Sar ester 74 as a prodrug that overcomes some of the pharmaceuticals and absorption-related limitations associated with 1. The design of 74 takes advantage of a self-immolative process of drug release in which cyclization of the promoiety to a diketopiperazine occurs at neutral pH and is facilitated by the presence of a sarcosine linker to exert

conformational bias toward the presence of the *cis*-amide conformation. Oral dosing of **74** to rats provided a four-fold improved exposure and an eight-fold improved C_{24h} value of **1** compared with an equivalent dose of the parent drug with the observation of only very low levels of circulating prodrug. In a dose escalation study, a dose-proportional increase in both plasma concentration and trough concentration of **1** was observed following oral administration of **74** at doses of up to 30 mg/kg. While the performance and profile of **74** in rats is encouraging, realization of its full potential as a delivery vehicle for **1** will require additional PK studies in higher species to more fully understand the relevance to human exposure predictions. The pH-activatable immolative prodrug design described herein appears to offer a viable strategy for facilitating the activation of prodrugs to release the parent drugs in those circumstances where hydrolytic enzymes may have difficulty in accessing the promoiety because of the steric hindrance presented by structural elements embedded in the parent molecule and may have broader applications.

EXPERIMENTAL SECTION

Details of materials and general methods are provided in the Supporting Information. The analytical purity of the compounds was assessed by HPLC analysis and determined to be $\geq 95\%$, unless otherwise noted. The following HPLC methods were used to determine the analytical purity of the compounds.

(i) Analytical HPLC method A: column = Sunfire C18 [150 \times 4.6 mm] 3.5 μm ; buffer = 0.05% $\text{CF}_3\text{CO}_2\text{H}$ in H_2O ; mobile phase A = buffer/MeCN [95:5]; mobile phase B = MeCN/buffer [95:5]; 10% B to 100% B; run time = 23 min; flow rate = 1.0 mL/min).

(ii) Analytical HPLC method B: column = XBridge phenyl C18 [150 \times 4.6 mm] 3.5 μm ; buffer = 0.05% $\text{CF}_3\text{CO}_2\text{H}$ in H_2O ; mobile phase A = buffer/MeCN [95:5]; mobile phase B = MeCN/buffer [95:5]; 10% B to 100% B; run time = 23 min; flow rate = 1.0 mL/min).

(iii) Analytical HPLC method C: column = Kinetex Evo C18 [100 \times 4.6 mm] 2.6 μm ; buffer = 0.05% $\text{CF}_3\text{CO}_2\text{H}$ in H_2O ; mobile phase A = buffer/MeCN [95:5]; mobile phase B = MeCN/buffer [95:5]; 10% B to 100% B; run time = 23 min; flow rate = 1.0 mL/min).

(iv) Analytical HPLC method D: column = Kinetex Biphenyl C18 [100 \times 4.6 mm] 2.6 μm ; buffer = 0.05% $\text{CF}_3\text{CO}_2\text{H}$ in H_2O ; mobile phase A = buffer/MeCN [95:5]; mobile phase B = MeCN/buffer [95:5]; 10% B to 100% B; run time = 23 min; flow rate = 1.0 mL/min).

Experimental Procedures. *Methyl ((5S,8S,9S,14S)-8-Benzyl-5-(tert-butyl)-15,15-dimethyl-3,6,13-trioxo-9-(phosphonoxy)-11-(4-(pyridin-2-yl)benzyl)-2-oxa-4,7,11,12-tetraazahexadecan-14-yl)carbamate (2)*. To a stirred solution of **9** (200 mg, 0.21 mmol) in $\text{ClCH}_2\text{CH}_2\text{Cl}$ (5 mL) were added $\text{CF}_3\text{CO}_2\text{H}$ (2 mL, 26.0 mmol) and anisole (0.2 mL, 1.83 mmol). The reaction mixture was stirred at room temperature for 16 h, concentrated under high vacuum at 30 $^\circ\text{C}$ to leave a colorless gum. The crude product was purified using RP-HPLC (column: Sunfire C18 (19 \times 150 mm) 5 μm ; mobile phase A: 0.1% $\text{CF}_3\text{CO}_2\text{H}$ in H_2O ; mobile phase B: CH_3CN ; flow rate: 20 mL/min; gradient (T/%B): 0/10, 10/50). The pooled HPLC fractions were concentrated using high vacuum at 30 $^\circ\text{C}$. The residue was dissolved in a mixture of CH_3CN and H_2O , frozen, and lyophilized for 12 h to afford the title compound as a white solid (120 mg, 0.150 mmol, 72% yield). ^1H NMR (400 MHz, $\text{DMSO}-d_6$): δ 9.77–9.63 (m, 1H), 8.81–8.64 (m, 1H), 8.11–7.99 (m, 2H), 7.95–7.86 (m, 2H), 7.85–7.77 (m, 1H), 7.64–7.54 (m, 2H), 7.52–7.43 (m, 1H), 7.30–7.10 (m, 5H), 6.85–6.63 (m, 2H), 4.75–4.57 (m, 1H), 4.34–4.10 (m, 2H), 4.03–3.89 (m, 1H), 3.73–3.59 (m, 2H), 3.57–3.53 (m, 3H), 3.43–3.26 (m, 3H), 3.02–2.71 (m, 4H), 0.93–0.57 (m, 18H); LCMS (ES) m/z : 785.2 [M + H] $^+$. Analytical HPLC-RT and purity:

method C = 6.40 min and 99.60% method D = 5.16 min and 99.80%; HRMS (ESI/Orbitrap) m/z : [M + H] $^+$ calcd for $\text{C}_{38}\text{H}_{54}\text{N}_6\text{O}_{10}\text{P}$, 785.3634; found, 785.3622.

Methyl ((5S,8S,9S,14S)-8-Benzyl-9-((bis(benzyloxy)phosphoryl)oxy)-5-(tert-butyl)-15,15-dimethyl-3,6,13-trioxo-11-(4-(pyridin-2-yl)benzyl)-2-oxa-4,7,11,12-tetraazahexadecan-14-yl)carbamate (9). To a stirred solution of **1** (1 g, 1.42 mmol) in CH_3CN (15 mL) were added tetrazole (0.099 g, 1.42 mmol) and dibenzyl diisopropylphosphoramidite (0.72 mL, 2.13 mmol). The reaction mixture was stirred at room temperature for 8 h and cooled to 0 $^\circ\text{C}$, and an aqueous solution of H_2O_2 (0.222 mL, 2.84 mmol) was added. The reaction mixture was stirred at 0 $^\circ\text{C}$ for 10 min and then partitioned between EtOAc and H_2O . The organic layer was washed with 10% aqueous Na_2CO_3 solution and brine, dried over anhydrous Na_2SO_4 , filtered, and concentrated under vacuum to afford a colorless oil. The crude product was purified by preparative HPLC (column: YMC TRIAT (20 \times 250 mm) 5 μm ; mobile phase A: 10 mM NH_4OAc in H_2O ; mobile phase B: CH_3CN ; flow rate: 20 mL/min; gradient (T/%B): 0/60, 2/60, 15/80). The pooled HPLC fractions were concentrated under reduced pressure below 30 $^\circ\text{C}$. The residue was dissolved in a mixture of CH_3CN and H_2O , frozen, and lyophilized for 12 h to obtain the title product as an off-white solid (900 mg, 62.4%). ^1H NMR (400 MHz, $\text{CH}_3\text{OH}-d_3$): δ 8.63–8.56 (m, 1H), 7.90–7.85 (m, 1H), 7.84–7.77 (m, 3H), 7.84–7.76 (m, 3H), 7.76–7.70 (m, 1H), 7.48–7.42 (m, 2H), 7.40–7.34 (m, 11H), 7.24–7.14 (m, 4H), 6.57–6.46 (m, 1H), 5.17–5.07 (m, 4H), 4.64–4.53 (m, 1H), 4.19–4.08 (m, 1H), 4.00–3.89 (m, 2H), 3.72–3.60 (m, 4H), 3.55–3.45 (m, 4H), 3.24–3.13 (m, 2H), 2.95–2.75 (m, 2H), 1.02–0.56 (m, 18H); LCMS (ES) m/z : 965.5 [M + H] $^+$.

Methyl ((5S,8S,9S,14S)-8-Benzyl-5-(tert-butyl)-15,15-dimethyl-9-((methylthio)methoxy)-3,6,13-trioxo-11-(4-(pyridin-2-yl)benzyl)-2-oxa-4,7,11,12-tetraazahexadecan-14-yl)carbamate (10). Acetic anhydride (1.34 mL, 14.2 mmol) and $\text{CH}_3\text{CO}_2\text{H}$ (2.44 mL, 42.6 mmol) were added to a stirred solution of **1** (1.0 g, 1.42 mmol) in DMSO (2.6 mL, 36.9 mmol). The homogeneous reaction mixture was stirred at room temperature for 2 days before being partitioned between EtOAc and H_2O . The organic layer was washed with 10% aqueous Na_2CO_3 solution followed by brine solution and dried over Na_2SO_4 , filtered, and concentrated under reduced pressure to afford 2.1 g of crude compound, which was divided into two equal portions. The first half was triturated with Et_2O , the solid filtered, washed with Et_2O , and dried under vacuum to afford 600 mg as an off white solid. The second half was purified by reversed phase HPLC (column: Sunfire C18 (150 \times 19 mm) 5 μm ; mobile phase A: 10 mM NH_4OAc in H_2O ; mobile phase B: $\text{CH}_3\text{CN}/i\text{PrOH}$ (70:30); flow rate: 20 mL/min; gradient: 0/40, 2/40, 17/70). The pooled HPLC fractions were concentrated under high vacuum below 30 $^\circ\text{C}$. The residue was dissolved in a mixture of CH_3CN and H_2O ; the solution was frozen and lyophilized for 16 h to afford 260 mg of an off white solid. The combined title product was obtained as an off white solid (860 mg, 1.13 mmol, 79% yield). ^1H NMR (400 MHz, $\text{DMSO}-d_6$): δ 8.98 (s, 1H), 8.71–8.59 (m, 1H), 7.97 (d, J = 8.5 Hz, 2H), 7.94–7.90 (m, 1H), 7.86 (dt, J = 2.0, 7.8 Hz, 1H), 7.60 (br d, J = 9.0 Hz, 1H), 7.41 (d, J = 8.5 Hz, 2H), 7.33 (ddd, J = 1.5, 4.8, 7.3 Hz, 1H), 7.25–7.08 (m, 5H), 6.81 (br d, J = 9.0 Hz, 1H), 6.63 (br d, J = 9.5 Hz, 1H), 5.11 (br d, J = 11.5 Hz, 1H), 4.90 (d, J = 11.5 Hz, 1H), 4.31 (br s, 1H), 4.01–3.83 (m, 3H), 3.78 (br s, 1H), 3.69 (br d, J = 9.5 Hz, 1H), 3.52 (d, J = 6.0 Hz, 6H), 2.95–2.79 (m, 3H), 2.78–2.71 (m, 1H), 2.17 (s, 3H), 0.76 (m, 18H); LCMS (ES) m/z : 765.4 [M + H] $^+$. Analytical HPLC-RT and purity: method C = 4.64 min and 99.60% method D = 6.13 min and 99.5%; HRMS (ESI/Orbitrap) m/z : [M + H] $^+$ calcd for $\text{C}_{40}\text{H}_{57}\text{N}_6\text{O}_9\text{S}$, 765.9905; found, 765.3977.

Disodium Methyl ((5S,8S,9S,14S)-8-Benzyl-5-(tert-butyl)-15,15-dimethyl-3,6,13-trioxo-9-((phosphonoxy)methoxy)-11-(4-(pyridin-2-yl)benzyl)-2-oxa-4,7,11,12-tetraazahexadecan-14-yl)carbamate (11). Powdered 4 Å molecular sieves (200.0 mg) and phosphoric acid (0.027 mL, 0.52 mmol) were added to a stirred solution of **10** (0.08 g, 0.105 mmol) in THF (3.0 mL). The mixture was cooled to 0 $^\circ\text{C}$, NIS (0.035 g, 0.157 mmol) was added, and the mixture was stirred at room temperature for 30 min. CH_3OH was added followed by 1.0 M $\text{Na}_2\text{S}_2\text{O}_3$ solution until the reaction mixture

became colorless. The pH of the mixture was adjusted to 10 with solid Na_2CO_3 and filtered. The filtrate was concentrated under reduced pressure to afford a residue which was dissolved in a mixture of CH_3CN and H_2O , frozen, and lyophilized for 16 h. The crude material was purified by using reversed phase preparative HPLC (column: X-Bridge phenyl (250 × 19 mm) 5 μm ; mobile phase A: Milli-Q H_2O ; mobile phase B: CH_3CN ; flow rate: 20 mL/min; gradient: 0/10, 10/30). The pooled HPLC fractions were concentrated under high vacuum below 30 °C. The residue was dissolved in a mixture of CH_3CN and H_2O , frozen, and lyophilized for 16 h to afford the title compound as an off white solid (42 mg, 0.048 mmol, 45% yield). ^1H NMR (400 MHz, D_2O): δ 8.66–8.55 (m, 1H), 8.23–8.16 (m, 1H), 8.06–7.97 (m, 1H), 7.83–7.74 (m, 2H), 7.70–7.51 (m, 3H), 7.31–7.14 (m, 5H), 5.26–5.03 (m, 2H), 4.61–4.43 (m, 1H), 4.08–3.96 (m, 1H), 3.91–3.72 (m, 2H), 3.68 (s, 3H), 3.58–3.46 (m, 2H), 3.43 (s, 3H), 3.02–2.75 (m, 4H), 0.82–0.80 (m, 18H). LCMS (ES) m/z : 815.2 [M + H]⁺. Analytical HPLC-RT and purity: method C = 4.10 min and 99.30% method D = 5.22 min and 98.8%; HRMS (ESI/Orbitrap) m/z : [M + H]⁺ calcd for $\text{C}_{39}\text{H}_{56}\text{N}_6\text{O}_{11}\text{P}$, 815.3739; found, 815.3726.

(R)-(5S,10S,11S,14S)-11-Benzyl-5,14-di-tert-butyl-3,6,13,16-tetraoxo-8-(4-(pyridin-2-yl)benzyl)-2,17-dioxo-4,7,8,12,15-pentaoxaoctadecan-10-yl 2-((tert-Butoxycarbonyl)amino)-3-methylbutanoate (22). (R)-2-((tert-Butoxycarbonyl)amino)-3-methylbutanoic acid (0.055 g, 0.255 mmol), DCC (0.088 g, 0.426 mmol), and DMAP (5.2 mg, 0.043 mmol) were added to a solution of 1 (0.150 g, 0.213 mmol) in CH_2Cl_2 (10 mL), and the reaction mixture was stirred at RT overnight before adding H_2O (1 × 50 mL). The mixture was extracted with CH_2Cl_2 (3 × 50 mL), the combined organic layer was dried over anhydrous Na_2SO_4 , filtered, and concentrated to afford an off-white solid (250 mg). The crude material was purified by preparative HPLC (column: XBridge phenyl C18 (19 × 150 mm) 5 μm ; mobile phase A: 10 mM NH_4OAc in H_2O ; mobile phase B: CH_3CN ; flow rate: 16 mL/min; gradient: 80% isocratic mobile phase B in mobile phase A in 20 min). The pooled HPLC fractions were concentrated under reduced pressure below 30 °C. The residue was dissolved in a mixture of CH_3CN and H_2O ; the solution was frozen and lyophilized for 12 h to obtain the title product as an off-white solid (45 mg, 23%). ^1H NMR (400 MHz, $\text{DMSO}-d_6$): δ 8.81 (br s, 1H), 8.65 (td, J = 2.5, 1.0 Hz, 1H), 7.95–7.81 (m, 5H), 7.36–7.30 (m, 3H), 7.23–7.12 (m, 6H), 6.70 (dd, J = 9.0, 5.0 Hz, 2H), 4.99 (t, J = 6.5 Hz, 1H), 4.69 (br s, 1H), 4.16 (dd, J = 8.8, 5.8 Hz, 1H), 4.02–3.93 (m, 3H), 3.65 (d, J = 9.5 Hz, 1H), 3.56 (s, 3H), 3.42 (s, 3H), 3.03–2.87 (m, 2H), 2.67 (dt, J = 4.0, 2.0 Hz, 2H), 2.19–2.09 (m, 1H), 1.41 (s, 9H), 0.94 (d, J = 7.0 Hz, 6H), 0.86 (s, 9H), 0.76 (s, 9H); LCMS (ES): m/z : 904.4 [M + H]⁺; analytical HPLC-RT and purity: method B = 9.839 min and 99.67%.

(R)-(5S,10S,11S,14S)-11-Benzyl-5,14-di-tert-butyl-3,6,13,16-tetraoxo-8-(4-(pyridin-2-yl)benzyl)-2,17-dioxo-4,7,8,12,15-pentaoxaoctadecan-10-yl 2-((tert-Butoxycarbonyl)amino)-3-methylbutanoate Dihydrochloride (24). A solution of 4 M HCl in Et_2O solution (0.134 mL, 4.42 mmol) was added to 22 (0.040 g, 0.044 mmol) in a 5 mL round-bottom flask cooled to 0 °C. The reaction mixture was stirred at RT for 1 h before being concentrated under vacuum. The residue was dissolved in a mixture of CH_3CN and H_2O ; the solution was frozen and lyophilized for 12 h to obtain the title product as a light yellow solid (35 mg; 88%). ^1H NMR (400 MHz, $\text{DMSO}-d_6$): δ 9.06 (s, 1H), 8.72 (d, J = 4.5 Hz, 1H), 8.60 (br s, 3H), 8.15–8.03 (m, 2H), 7.99–7.92 (m, 3H), 7.54 (br s, 1H), 7.43 (d, J = 8.0 Hz, 2H), 7.26–7.12 (m, 5H), 6.75 (d, J = 10.0 Hz, 1H), 6.68 (d, J = 9.5 Hz, 1H), 5.17 (t, J = 6.5 Hz, 1H), 4.06–3.90 (m, 5H), 3.68–3.62 (m, 1H), 3.55 (s, 3H), 3.41 (s, 3H), 3.05–2.90 (m, 2H), 2.78–2.65 (m, 2H), 2.36–2.26 (m, 1H), 1.10–1.05 (m, 6H), 0.83 (s, 9H), 0.76 (s, 9H); LCMS (ES) m/z : 804.4 [M + H]⁺; analytical HPLC-RT and purity: method A = 6.015 min and 99.04% method B = 7.144 min and 97.75%; HRMS (ESI/Orbitrap) m/z : [M + H]⁺ calcd for $\text{C}_{43}\text{H}_{61}\text{N}_7\text{O}_8$, 804.4654; found, 804.4661.

(S)-(5S,10S,11S,14S)-11-Benzyl-5,14-di-tert-butyl-3,6,13,16-tetraoxo-8-(4-(pyridin-2-yl)benzyl)-2,17-dioxo-4,7,8,12,15-pentaoxaoctadecan-10-yl 2-((S)-2-((tert-Butoxycarbonyl)amino)-3-methylbutanamido)-3-methylbutanoate (25). (S)-2-((tert-Butoxycarbonyl)amino)-3-methylbutanoic acid (0.041 g, 0.187

mmol), DIPEA (0.109 mL, 0.622 mmol) and HATU (0.047 g, 0.124 mmol) was added to a solution of 23 (0.100 g, 0.124 mmol) in DMF (10 mL), and the mixture was stirred overnight at RT. H_2O (1 × 50 mL) was added, and the mixture was extracted with EtOAc (3 × 50 mL). The combined organic layer was washed with brine (1 × 50 mL), dried over anhydrous Na_2SO_4 , filtered, and concentrated to leave a gum (150 mg). The crude compound was purified by preparative HPLC (column: XBridge phenyl (20 × 250 mm) 5 μm ; mobile phase A: 10 mM NH_4OAc in H_2O ; mobile phase B: CH_3CN ; flow rate: 17 mL/min; gradient: 30–70% mobile phase B in mobile phase A in 10 min). The pooled HPLC fractions were concentrated under reduced pressure below 30 °C. The solid residue was dissolved in a mixture of CH_3CN and H_2O ; the solution was frozen and lyophilized for 12 h to obtain the title product as an off-white solid (60 mg, 45%). ^1H NMR (300 MHz, $\text{DMSO}-d_6$): δ 8.88–8.78 (m, 1H), 8.68–8.60 (m, 1H), 8.00–7.79 (m, 6H), 7.38–7.26 (m, 3H), 7.17 (s, 5H), 6.88–6.77 (m, 1H), 6.74–6.62 (m, 2H), 5.08–4.97 (m, 1H), 4.72–4.61 (m, 1H), 4.55–4.45 (m, 1H), 4.05–3.79 (m, 4H), 3.69–3.61 (m, 1H), 3.56 (s, 3H), 3.42 (s, 3H), 3.04–2.85 (m, 2H), 2.75–2.55 (m, 2H), 2.24–2.08 (m, 1H), 2.02–1.91 (m, 1H), 1.38 (s, 9H), 0.95 (s, 6H), 0.90–0.70 (m, 24H); LCMS (ES) m/z : 1003.4 [M + H]⁺; analytical HPLC-RT and purity: method B = 10.542 min and 94.69%.

(S)-(5S,10S,11S,14S)-11-Benzyl-5,14-di-tert-butyl-3,6,13,16-tetraoxo-8-(4-(pyridin-2-yl)benzyl)-2,17-dioxo-4,7,8,12,15-pentaoxaoctadecan-10-yl 2-((S)-2-Amino-3-methylbutanamido)-3-methylbutanoate Dihydrochloride (29). A solution of 4 M HCl in Et_2O (0.15 mL, 4.98 mmol) was added to 25 (0.050 g, 0.050 mmol) in a 5 mL round-bottom flask cooled to 0 °C. The mixture was allowed to warm to RT and stirred for 1 h before being concentrated under vacuum. The residue was dissolved in a mixture of CH_3CN and H_2O ; the solution was frozen and lyophilized for 12 h to obtain the title product as light yellow solid (38 mg; 76%). ^1H NMR (400 MHz, D_2O): δ 8.71 (d, J = 5.5 Hz, 1H), 8.60 (t, J = 7.8 Hz, 1H), 8.27 (d, J = 8.3 Hz, 1H), 7.97 (t, J = 6.8 Hz, 1H), 7.76 (d, J = 8.3 Hz, 2H), 7.62 (d, J = 8.0 Hz, 2H), 7.29–7.16 (m, 5H), 4.98 (br s, 1H), 4.35 (d, J = 6.8 Hz, 1H), 4.06 (d, J = 12.8 Hz, 1H), 3.90 (d, J = 5.8 Hz, 1H), 3.87–3.77 (m, 2H), 3.64 (s, 3H), 3.52–3.43 (m, 2H), 3.33 (br s, 3H), 3.03–2.93 (m, 1H), 2.91–2.80 (m, 2H), 2.75–2.73 (m, 1H), 2.28–2.12 (m, 2H), 1.06–0.96 (m, 12H), 0.83 (s, 9H), 0.66 (s, 9H); LCMS (ES) m/z : 903.9 [M + H]⁺; analytical HPLC-RT and purity: method A = 6.351 min and 97.53% method B = 6.923 min and 97.50%; HRMS (ESI/Orbitrap) m/z : [M + H]⁺ calcd for $\text{C}_{48}\text{H}_{70}\text{N}_8\text{O}_9$, 903.5339; found, 903.5330.

(5S,10S,11S,14S)-11-Benzyl-5,14-di-tert-butyl-3,6,13,16-tetraoxo-8-(4-(pyridin-2-yl)benzyl)-2,17-dioxo-4,7,8,12,15-pentaoxaoctadecan-10-yl 2-((tert-Butoxycarbonyl)amino)acetic acid (34). 2-((tert-Butoxycarbonyl)amino)acetic acid (0.045 g, 0.255 mmol), DCC (0.088 g, 0.426 mmol), and DMAP (5.20 mg, 0.043 mmol) were added to a solution of 1 (0.150 g, 0.213 mmol) in CH_2Cl_2 (20 mL), and the mixture was stirred for 14 h at RT. H_2O (1 × 50 mL) was added, and the mixture was extracted with CH_2Cl_2 (3 × 50 mL). The combined organic layer was dried over anhydrous Na_2SO_4 , filtered, and concentrated to leave an off-white solid. The crude compound was purified by preparative HPLC (column: XBridge phenyl (19 × 250 mm) 5 μm ; mobile phase A: 10 mM NH_4OAc in H_2O ; mobile phase B: CH_3CN ; flow rate: 18 mL/min; gradient: 30–60% mobile phase B in mobile phase A in 8 min). The pooled HPLC fractions were concentrated under reduced pressure below 30 °C; the residual solid was dissolved in a mixture of CH_3CN and H_2O , frozen, and lyophilized for 12 h to obtain the title product as an off-white solid (140 mg, 76%). ^1H NMR (400 MHz, $\text{DMSO}-d_6$) δ 8.96 (s, 1H), 8.69–8.58 (m, 1H), 7.99–7.78 (m, 5H), 7.41–7.28 (m, 3H), 7.27–7.09 (m, 6H), 6.73–6.60 (m, 2H), 5.07 (t, J = 5.8 Hz, 1H), 4.52 (br s, 1H), 4.05–3.91 (m, 3H), 3.88 (d, J = 6.0 Hz, 1H), 3.84–3.71 (m, 1H), 3.66 (d, J = 9.5 Hz, 1H), 3.55 (s, 3H), 3.43 (s, 3H), 3.07 (dd, J = 13.3, 5.8 Hz, 1H), 2.91 (dd, J = 13.1, 7.5 Hz, 1H), 2.76–2.57 (m, 2H), 1.41 (s, 9H), 0.81 (s, 9H), 0.74 (s, 9H); LCMS (ES) m/z : 861.4 [M + H]⁺; analytical HPLC-RT and purity: method B = 9.011 min and 99.83%.

(5*S*,10*S*,11*S*,14*S*)-11-Benzyl-5,14-di-*tert*-butyl-3,6,13,16-tetraoxo-8-(4-(pyridin-2-yl)benzyl)-2,17-dioxo-4,7,8,12,15-pentaoxaoctadecan-10-yl 2-((*tert*-Butoxycarbonyl)(methyl)amino)acetate (**35**). 2-((*tert*-Butoxycarbonyl)(methyl)amino)acetic acid (268 mg, 1.419 mmol), DMAP (87 mg, 0.709 mmol), and DCC (293 mg, 1.419 mmol) were added to a solution of **1** (500 mg, 0.709 mmol) in CH₂Cl₂ (10 mL), and the mixture was stirred overnight at RT. The mixture was concentrated under vacuum, and the residue was purified by preparative HPLC. The pooled HPLC fractions were concentrated under reduced pressure below 30 °C, the residual solid was dissolved in a mixture of CH₃CN and H₂O, frozen, and lyophilized for 12 h to obtain the title product as a white solid (400 mg; 64%). ¹H NMR (400 MHz, MeOD): δ 8.64–8.57 (m, 1H), 7.97–7.78 (m, 5H), 7.50 (d, *J* = 8.5 Hz, 2H), 7.41–7.33 (m, 1H), 7.24 (s, 5H), 5.31–5.17 (m, 1H), 4.69–4.50 (m, 1H), 4.32–3.91 (m, 5H), 3.77–3.49 (m, 7H), 3.12–2.99 (m, 5H), 2.97–2.84 (m, 1H), 2.79–2.62 (m, 1H), 1.50 (d, *J* = 19.6 Hz, 9H), 0.96–0.76 (m, 18H); LCMS (ES) *m/z*: 877.4 [M + H]⁺; analytical HPLC-RT and purity: method B = 9.689 min and 99.53%.

(5*S*,10*S*,11*S*,14*S*)-11-Benzyl-5,14-di-*tert*-butyl-3,6,13,16-tetraoxo-8-(4-(pyridin-2-yl)benzyl)-2,17-dioxo-4,7,8,12,15-pentaoxaoctadecan-10-yl 2-((*tert*-Butoxycarbonyl)amino)-3-phenylpropanoate (**42**). (S)-2-((*tert*-Butoxycarbonyl)amino)-3-phenylpropanoic acid (0.059 g, 0.221 mmol), DCC (0.076 g, 0.369 mmol), and DMAP (4.51 mg, 0.037 mmol) were added to a solution of **1** (0.130 g, 0.184 mmol) in CH₂Cl₂ (15 mL), and the mixture was stirred at RT for 16 h. H₂O was added (1 × 50 mL), the mixture was extracted with EtOAc (3 × 50 mL), and the combined organic layer was washed with brine (1 × 50 mL), dried over anhydrous Na₂SO₄, filtered, and concentrated to leave an off-white solid. The crude compound was purified by preparative HPLC (column: Sunfire C18 (19 × 150 mm) 5 μm; mobile phase A: 10 mM NH₄OAc in H₂O; mobile phase B: CH₃CN; flow rate: 18 mL/min; gradient: 50–70% mobile phase B in mobile phase A in 8 min). The pooled HPLC fractions were concentrated under reduced pressure below 30 °C, the residual solid was dissolved in a mixture of CH₃CN and H₂O; the solution was frozen and lyophilized for 12 h to obtain the title product as an off-white solid (130 mg, 74%). ¹H NMR (400 MHz, DMSO-*d*₆): δ 8.89 (s, 1H), 8.65 (dd, *J* = 6.5, 1.0 Hz, 1H), 7.93 (d, *J* = 8.0 Hz, 2H), 7.91–7.82 (m, 2H), 7.70 (d, *J* = 10.0 Hz, 1H), 7.38 (d, *J* = 8.0 Hz, 2H), 7.35–7.26 (m, 6H), 7.25–7.12 (m, 6H), 6.72 (d, *J* = 10.0 Hz, 1H), 6.66 (d, *J* = 9.0 Hz, 1H), 5.02 (br s, 1H), 4.61 (br s, 1H), 4.35 (br s, 1H), 4.00 (t, *J* = 11.0 Hz, 3H), 3.67 (d, *J* = 9.0 Hz, 1H), 3.54 (s, 3H), 3.43 (s, 3H), 3.26 (d, *J* = 4.5 Hz, 1H), 3.12–3.03 (m, 1H), 3.01–2.85 (m, 2H), 2.73–2.58 (m, 2H), 1.32 (s, 9H), 0.87 (s, 9H), 0.74 (s, 9H); LCMS (ES) *m/z*: 952.9 [M + H]⁺. Analytical HPLC-RT and purity: method A = 17.030 min and 99.76% method B = 18.399 min and 99.83%.

(5*S*,10*S*,11*S*,14*S*)-11-Benzyl-5,14-di-*tert*-butyl-3,6,13,16-tetraoxo-8-(4-(pyridin-2-yl)benzyl)-2,17-dioxo-4,7,8,12,15-pentaoxaoctadecan-10-yl 2-Aminoacetate Dihydrochloride (**44**). A solution of 4 M HCl in dioxane (0.441 mL, 14.50 mmol) was added to **34** (0.125 g, 0.145 mmol) in a 5 mL round-bottom flask maintained at 0 °C. The mixture was stirred for 1 h at RT before being concentrated under vacuum. The residue was dissolved in a mixture of CH₃CN and H₂O; the solution was frozen and lyophilized for 12 h to obtain the title product as a light yellow solid (110 mg; 89%). ¹H NMR (400 MHz, DMSO-*d*₆): δ 9.19 (s, 1H), 8.77 (d, *J* = 4.5 Hz, 1H), 8.59 (br s, 3H), 8.25 (br s, 1H), 8.16 (d, *J* = 8.0 Hz, 1H), 8.02–7.93 (m, 3H), 7.66 (br s, 1H), 7.48 (d, *J* = 8.0 Hz, 2H), 7.28–7.11 (m, 5H), 6.71 (d, *J* = 9.5 Hz, 1H), 6.75 (d, *J* = 9.5 Hz, 1H), 5.16 (t, *J* = 6.5 Hz, 1H), 4.65 (br s, 1H), 4.06–3.88 (m, 2H), 3.75–3.62 (m, 2H), 3.56 (s, 3H), 3.53–3.44 (m, 2H), 3.40 (s, 3H), 3.07–2.90 (m, 2H), 2.79–2.64 (m, 2H), 0.82 (s, 9H), 0.75 (s, 9H); LCMS (ES) *m/z*: 762.4 [M + H]⁺; analytical HPLC-RT and purity: method A = 5.954 min and 99.11% method B = 6.730 min and 99.08%. HRMS (ESI/Orbitrap) *m/z*: [M + H]⁺ calcd for C₄₀H₅₅N₇O₈, 762.4185; found, 762.4193.

(5*S*,10*S*,11*S*,14*S*)-11-Benzyl-5,14-di-*tert*-butyl-3,6,13,16-tetraoxo-8-(4-(pyridin-2-yl)benzyl)-2,17-dioxo-4,7,8,12,15-pentaoxaoctadecan-10-yl 2-(Methylamino)acetate Dihydrochloride (**45**).

A solution of 4 M HCl in dioxane (1.0 mL, 32.9 mmol) was added to **35** (0.2 g, 0.228 mmol) in a 5 mL round-bottom flask maintained at 0 °C. The reaction mixture was warmed to RT and stirred for 2 h before being concentrated under vacuum. The residue was triturated with Et₂O and the ethereal layer decanted. The residual solid was dissolved in a mixture of CH₃CN and H₂O, frozen, and lyophilized for 12 h to obtain the title product as a white solid (38 mg; 19%). ¹H NMR (400 MHz, DMSO) δ = 9.45–9.25 (m, 2H), 9.18–9.06 (m, 1H), 8.81–8.62 (m, 1H), 7.98–7.96 (m, 5H), 7.54–7.39 (m, 3H), 7.21 (br s, 5H), 6.84–6.61 (m, 2H), 5.25–5.11 (m, 1H), 4.63–4.50 (m, 1H), 4.13–3.89 (m, 5H), 3.68–3.62 (m, 1H), 3.55–3.50 (m, 3H), 3.42 (s, 3H), 3.08–2.89 (m, 2H), 2.69 (s, 5H), 0.85 (s, 9H), 0.75 (s, 9H); LCMS (ES) *m/z*: 776.4 [M + H]⁺; analytical HPLC-RT and purity: method A = 5.886 min and 98.13% method B = 6.902 min and 98.94%. HRMS (ESI/Orbitrap) *m/z*: [M + H]⁺ calcd for C₄₁H₅₇N₇O₈, 776.4341; found, 776.4343.

(5*S*,10*S*,11*S*,14*S*)-11-Benzyl-5,14-di-*tert*-butyl-3,6,13,16-tetraoxo-8-(4-(pyridin-2-yl)benzyl)-2,17-dioxo-4,7,8,12,15-pentaoxaoctadecan-10-yl 2-Amino-3-phenylpropanoate, Dihydrochloride (**53**). A solution of 4 M HCl in dioxane (4.47 mL, 147 mmol) was added to **42** (2.800 g, 2.94 mmol) in a round-bottom flask maintained at 0 °C. The reaction mixture was warmed to RT and stirred for 1 h before being concentrated under vacuum. The residue was dissolved in a mixture of CH₃CN and H₂O, and the solution was frozen and lyophilized for 12 h to obtain the title product as an off-white solid (2.50 g; 85%). ¹H NMR (400 MHz, DMSO-*d*₆): δ 9.20 (s, 1H), 8.82 (br s, 3H), 8.74 (d, *J* = 4.5 Hz, 1H), 8.17 (br s, 1H), 8.14–8.07 (m, 1H), 7.97 (d, *J* = 8.5 Hz, 2H), 7.91 (d, *J* = 9.5 Hz, 1H), 7.60 (br s, 1H), 7.47 (d, *J* = 8.0 Hz, 2H), 7.40–7.32 (m, 4H), 7.32–7.25 (m, 1H), 7.24–7.12 (m, 5H), 6.82 (d, *J* = 9.5 Hz, 1H), 6.72 (d, *J* = 10.0 Hz, 1H), 5.07 (t, *J* = 6.5 Hz, 1H), 4.74–4.65 (m, 1H), 4.38 (d, *J* = 5.5 Hz, 1H), 4.02–3.92 (m, 3H), 3.65 (d, *J* = 9.5 Hz, 1H), 3.53 (s, 3H), 3.41–3.32 (m, 4H), 3.29–3.21 (m, 1H), 3.01–2.88 (m, 2H), 2.67 (d, *J* = 7.0 Hz, 2H), 0.83 (s, 9H), 0.74 (s, 9H); LCMS (ES) *m/z*: 852.4 [M + H]⁺; analytical HPLC-RT and purity: method A = 6.879 min and 99.67% method B = 8.304 min and 99.65%. HRMS (ESI/Orbitrap) *m/z*: [M + H]⁺ calcd for C₄₇H₆₁N₇O₈, 852.4654; found, 852.4660.

(5*S*,10*S*,11*S*,14*S*)-11-Benzyl-5,14-di-*tert*-butyl-3,6,13,16-tetraoxo-8-(4-(pyridin-2-yl)benzyl)-2,17-dioxo-4,7,8,12,15-pentaoxaoctadecan-10-yl 2-((S)-2-Amino-N-methyl-3-phenylpropanamido)acetate, Dihydrochloride (**74**). A solution of 4 M HCl in dioxane (1 mL, 32.9 mmol) was added to **79** (65 mg, 0.064 mmol) in a 5 mL flask maintained at 0 °C. The reaction mixture was warmed to RT and stirred for 1 h before being concentrated under vacuum. The residue was triturated with Et₂O, the ethereal layer was decanted, and the residual solid was dried under vacuum. The solid was dissolved in a mixture of CH₃CN and H₂O, frozen, and lyophilized for 12 h to obtain the title product as white solid (63.95 mg; 98%). ¹H NMR (400 MHz, CH₃OH-*d*₆): δ 8.86–8.79 (m, 1H), 8.68–8.56 (m, 1H), 8.38–8.28 (m, 1H), 8.21–7.88 (m, 3H), 7.75–7.65 (m, 2H), 7.42–7.30 (m, 5H), 7.20–7.10 (m, 5H), 5.29–5.17 (m, 1H), 4.81–4.71 (m, 2H), 4.52–4.36 (m, 1H), 4.28–4.01 (m, 3H), 3.94 (s, 1H), 3.81–3.57 (m, 5H), 3.52 (s, 2H), 3.28–3.12 (m, 2H), 3.11–2.96 (m, 5H), 2.92–2.64 (m, 2H), 0.91–0.73 (m, 18H); LCMS (ES) *m/z*: 923.4 [M + H]⁺; HPLC-RT and purity: (a) method A = 7.199 min and 96.7%; (b) method B = 7.519 min and 96.9%. HRMS (ESI/Orbitrap) *m/z*: [M + H]⁺ calcd for C₅₀H₆₆N₈O₉, 923.5026; found, 923.5032.

(5*S*,10*S*,11*S*,14*S*)-11-Benzyl-5,14-di-*tert*-butyl-3,6,13,16-tetraoxo-8-(4-(pyridin-2-yl)benzyl)-2,17-dioxo-4,7,8,12,15-pentaoxaoctadecan-10-yl 2-((S)-2-((*tert*-Butoxycarbonyl)amino)-N-methyl-3-phenylpropanamido)acetate (**79**). To a stirred solution of **45** (0.2 g, 0.236 mmol) in DMF (8 mL), DIPEA (0.206 mL, 1.178 mmol) was added followed by HATU (0.134 g, 0.353 mmol) and Boc-Phe-OH (0.125 g, 0.471 mmol). The reaction mixture was stirred at RT for 8 h before being partitioned between H₂O and EtOAc. The organic layer was separated and washed with brine solution (1 × 25 mL), dried over Na₂SO₄, and concentrated under vacuum at 50 °C to leave the crude product which was purified by preparative HPLC. The pooled HPLC fractions were concentrated under reduced pressure

below 30 °C. The residual solid was dissolved in a mixture of CH₃CN and H₂O, frozen, and lyophilized for 12 h to obtain the title product as a white solid (0.2 g, 81%). ¹H NMR (400 MHz, DMSO): δ 9.06–8.94 (m, 1H), 8.68–8.60 (m, 1H), 8.01–7.79 (m, 5H), 7.42–7.30 (m, 4H), 7.30–7.22 (m, 3H), 7.20–7.13 (m, 6H), 7.09–6.97 (m, 1H), 6.73–6.62 (m, 2H), 5.28–5.05 (m, 1H), 4.89–4.64 (m, 1H), 4.56–4.40 (m, 2H), 4.32–4.08 (m, 2H), 4.01–3.86 (m, 3H), 3.70–3.52 (m, 3H), 3.45–3.40 (m, 4H), 3.13–3.05 (m, 2H), 3.00–2.96 (m, 1H), 2.91–2.70 (m, 4H), 2.68–2.60 (m, 1H), 1.33–1.22 (m, 9H), 0.84–0.68 (m, 18H) *m/z*: 1023.7 [M + H]⁺; HPLC-RT: (a) method B = 10.351 min.

■ ASSOCIATED CONTENT

● Supporting Information

The Supporting Information is available free of charge on the ACS Publications website at DOI: 10.1021/acs.jmedchem.9b00002.

Molecular formula strings (CSV)

Figures 3–11 and Table 13; experimental section (synthesis) = experimental procedures of prodrugs (23, 30, 31, 32, 46, 47, 48, 49, 51, 52, 54, 59, 64, 66, 71, 78, 81, and 82); details of in vitro and in vivo experiments = stability evaluation in aqueous buffer; stability evaluation in bio-relevant media; solubility evaluation in aqueous buffer; pharmacokinetic evaluation; ex vivo stability in whole blood; alkaline phosphatase assay: determination of prodrug cleavage rate in vitro; rat hepatocyte study with and without PMSF/ABT; procedure for UGT1A1 assay; antiviral assays (PDF)

■ AUTHOR INFORMATION

Corresponding Author

*E-mail: murugaiah.andappan@syngeneintl.com. Phone: +91-9731600213.

ORCID

Nicholas A. Meanwell: 0000-0002-8857-1515

Present Addresses

[¶]ViiV Healthcare, 36 East Industrial Road, Branford, CT 06405, USA.

[∇]Formulation Division, R&D, Dr. Reddy's Laboratories Ltd., Bachupally, Qutubullapur, Hyderabad, Telangana, 500090, India.

Notes

The authors declare no competing financial interest.

■ ACKNOWLEDGMENTS

We thank Drs. Ramakanth Sarabu, Arvind Mathur, and Percy Carter for their support and inspiration. We thank Drs. Punit Marathe, Michael Hageman, and Bruce Car for productive discussions. We acknowledge the Discovery Analytical Sciences team for the analytical support.

■ ABBREVIATIONS

ABT, 1-aminobenzotriazole; ADME, absorption distribution metabolism and excretion; ALP, alkaline phosphatase; APV, amprenavir; ATV, Atazanavir; BCRP, breast cancer resistance protein; BID, bis in die; BLQ, below limit of quantification; cART, combination anti-retroviral therapy; CYP, cytochrome P450; DMAc, dimethylacetamide; *N,N*-dimethyl-Gly, *N,N*-dimethylglycine; FaSSIF, fasted state simulated intestinal fluid; FDA, Federal Drug Administration; FeSSIF, fed state

simulated intestinal fluid; HBA, hydrogen bond acceptor; HBD, hydrogen bond donor; HPβCD, hydroxypropyl β-cyclodextrin; LPV, lopinavir; MRP, multi-drug resistant protein; NNRTI, non-nucleoside reverse transcriptase inhibitor; NRTI, nucleoside reverse transcriptase inhibitor; OATP, organic anion transporting polypeptide; OCT, organic cation transporter; PepT1, peptidase transporter 1; P-gp, P-glycoprotein; PI, protease inhibitor; PMSF, phenylmethylsulfonyl fluoride; POM, phosphonoxyethyl; PPI, proton pump inhibitor; PSA, polar surface area; QD, quaque die; rIALP, recombinant intestinal alkaline phosphatase; RLM, rat liver microsome; RTV, ritonavir; UGT1A1, uridine diphosphate glucuronosyltransferase 1A1; WHO, World Health Organization

■ REFERENCES

- (1) Cihlar, T.; Fordyce, M. Current status and prospects of HIV treatment. *Curr. Opin. Virol.* **2016**, *18*, 50–56.
- (2) Samji, H.; Cescon, A.; Hogg, R. S.; Modur, S. P.; Althoff, K. N.; Buchacz, K.; Burchell, A. N.; Cohen, M.; Gebo, K. A.; Gill, M. J.; Justice, A.; Kirk, G.; Klein, M. B.; Korthuis, P. T.; Martin, J.; Napravnik, S.; Rourke, S. B.; Sterling, T. R.; Silverberg, M. J.; Deeks, S.; Jacobson, L. P.; Bosch, R. J.; Kitahata, M. M.; Goedert, J. J.; Moore, R.; Gange, S. J. The North American AIDS Collaboration on Research and Design (NA-ACCORD) of leDEA. Closing the Gap: Increases in Life Expectancy Among Treated HIV-Positive Individuals in the United States and Canada. *PLoS One* **2013**, *8*, No. e81355.
- (3) Zhan, P.; Pannecouque, C.; De Clercq, E.; Liu, X. Anti-HIV Drug Discovery and Development: Current Innovations and Future Trends. *J. Med. Chem.* **2016**, *59*, 2849–2878.
- (4) Ghosh, A. K.; Osswald, H. L.; Prato, G. Recent Progress in the Development of HIV-1 Protease Inhibitors for the Treatment of HIV/AIDS. *J. Med. Chem.* **2016**, *59*, 5172–5208.
- (5) Midde, N. M.; Patters, B. J.; Rao, P.; Cory, T. J.; Kumar, S. Investigational Protease Inhibitors as Antiretroviral Therapies. *Expert Opin. Invest. Drugs* **2016**, *25*, 1189–1200.
- (6) Farajallah, A.; Bunch, R. T.; Meanwell, N. A. Discovery and Development of Atazanavir. *Antiviral Drugs*; John Wiley & Sons, Inc.: New Jersey, 2011; pp 1–17.
- (7) Günthard, H. F.; Saag, M. S.; Benson, C. A.; del Rio, C.; Eron, J. J.; Gallant, J. E.; Hoy, J. F.; Mugavero, M. J.; Sax, P. E.; Thompson, M. A.; Gandhi, R. T.; Landovitz, R. J.; Smith, D. M.; Jacobsen, D. M.; Volberding, P. A. Antiretroviral Drugs for Treatment and Prevention of HIV Infection in Adults: 2016 Recommendations of the International Antiviral Society-USA Panel. *JAMA* **2016**, *316*, 191–210.
- (8) Appendix B, Table 3. Characteristics of Protease Inhibitors. <https://aidsinfo.nih.gov/guidelines/htmltables/1/5482> (accessed March 23, 2018).
- (9) Kis, O.; Zastre, J. A.; Hoque, M. T.; Walmsley, S. L.; Bendayan, R. Role of Drug Efflux and Uptake Transporters in Atazanavir Intestinal Permeability and Drug-Drug Interactions. *Pharm. Res.* **2013**, *30*, 1050–1064.
- (10) Zhu, L.; Persson, A.; Mahnke, L.; Eley, T.; Li, T.; Xu, X.; Agarwala, S.; Dragone, J.; Bertz, R. Effect of Low-Dose Omeprazole (20 mg daily) on the Pharmacokinetics of Multiple-Dose Atazanavir with Ritonavir in Healthy Subjects. *J. Clin. Pharmacol.* **2011**, *51*, 368–377.
- (11) Zhang, L.; Wu, F.; Lee, S. C.; Zhao, H.; Zhang, L. pH-Dependent Drug-Drug Interactions for Weak Base Drugs: Potential Implications for New Drug Development. *Clin. Pharmacol. Ther.* **2014**, *96*, 266–277.
- (12) Klein, C. E.; Chiu, Y.-L.; Cai, Y.; Beck, K.; King, K. R.; Causemaker, S. J.; Doan, T.; Esslinger, H.-U.; Podsadecki, T. J.; Hanna, G. J. Effects of Acid-Reducing Agents on the Pharmacokinetics of Lopinavir/Ritonavir and Ritonavir-Boosted Atazanavir. *J. Clin. Pharmacol.* **2008**, *48*, 553–562.

- (13) Bertz, R. J.; Persson, A.; Chung, E.; Zhu, L.; Zhang, J.; McGrath, D.; Grasela, D. Pharmacokinetics and Pharmacodynamics of Atazanavir-Containing Antiretroviral Regimens, With or Without Ritonavir, in Patients Who Are HIV-Positive and Treatment-Naive. *Pharmacotherapy* **2013**, *33*, 284–294.
- (14) Furfine, E. S.; Baker, C. T.; Hale, M. R.; Reynolds, D. J.; Salisbury, J. A.; Searle, A. D.; Studenberg, S. D.; Todd, D.; Tung, R. D.; Spaltenstein, A. Preclinical Pharmacology and Pharmacokinetics of GW433908, a Water-Soluble Prodrug of the Human Immunodeficiency Virus Protease Inhibitor Amprenavir. *Antimicrob. Agents Chemother.* **2004**, *48*, 791–798.
- (15) DeGoey, D. A.; Grampovnik, D. J.; Flosi, W. J.; Marsh, K. C.; Wang, X. C.; Klein, L. L.; McDaniel, K. F.; Liu, Y.; Long, M. A.; Kati, W. M.; Molla, A.; Kempf, D. J. Water-Soluble Prodrugs of the Human Immunodeficiency Virus Protease Inhibitors Lopinavir and Ritonavir. *J. Med. Chem.* **2009**, *52*, 2964–2970.
- (16) Subbaiah, M. A. M.; Meanwell, N. A.; Kadow, J. F.; Subramani, L.; Annadurai, M.; Ramar, T.; Desai, S. D.; Sinha, S.; Subramanian, M.; Mandlekar, S.; Sridhar, S.; Padmanabhan, S.; Bhutani, P.; Arla, R.; Jenkins, S. M.; Krystal, M. R.; Wang, C.; Sarabu, R. Coupling of an Acyl Migration Prodrug Strategy with Bio-activation To Improve Oral Delivery of the HIV-1 Protease Inhibitor Atazanavir. *J. Med. Chem.* **2018**, *61*, 4176–4188.
- (17) FDA. Website: Atazanavir Documents. https://www.accessdata.fda.gov/drugsatfda_docs/nda/2003/21-567_Reyataz_BioPharmr_P1.pdf (accessed June 09, 2018).
- (18) Patel, M.; Mandava, N.; Gokulgandhi, M.; Pal, D.; Mitra, A. Amino Acid Prodrugs: An Approach to Improve the Absorption of HIV-1 Protease Inhibitor, Lopinavir. *Pharmaceuticals* **2014**, *7*, 433–452.
- (19) Jain, R.; Agarwal, S.; Mandava, N. K.; Sheng, Y.; Mitra, A. K. Interaction of Dipeptide Prodrugs of Saquinavir with Multidrug Resistance Protein-2 (MRP-2): Evasion of MRP-2 Mediated Efflux. *Int. J. Pharm.* **2008**, *362*, 44–51.
- (20) Jain, R.; Duvvuri, S.; Kansara, V.; Mandava, N. K.; Mitra, A. K. Intestinal Absorption of Novel-Dipeptide Prodrugs of Saquinavir in Rats. *Int. J. Pharm.* **2007**, *336*, 233–240.
- (21) Hamada, Y.; Matsumoto, H.; Yamaguchi, S.; Kimura, T.; Hayashi, Y.; Kiso, Y. Water-Soluble Prodrugs of Dipeptide HIV Protease Inhibitors Based on O→N Intramolecular Acyl Migration: Design, Synthesis and Kinetic Study. *Bioorg. Med. Chem.* **2004**, *12*, 159–170.
- (22) Corbett, A. H.; Kashuba, A. D. Fosamprenavir. Vertex Pharmaceuticals/GlaxoSmithKline. *Curr. Opin. Investig. Drugs* **2002**, *3*, 384–390.
- (23) Subbaiah, M. A. M.; Meanwell, N. A.; Kadow, J. F. Design Strategies in the Prodrugs of HIV-1 Protease Inhibitors to Improve the Pharmaceutical Properties. *Eur. J. Med. Chem.* **2017**, *139*, 865–883.
- (24) Harbeson, S. L.; Tung, R. D. Azapeptide Derivatives. U.S. Patent 8,158,805 B2, Apr 17, 2012.
- (25) Concert Pharmaceuticals, Inc.'s Patent Owner Preliminary Response. <https://www.concertpharma.com/wp-content/uploads/2017/07/Concert-IPR2017-01256-Patent-Owners-Preliminary-Response.pdf> (accessed Oct 6, 2018).
- (26) Clas, S.-D.; Sanchez, R. I.; Nofsinger, R. Chemistry-enabled drug delivery (prodrugs): recent progress and challenges. *Drug Discovery Today* **2014**, *19*, 79–87.
- (27) Rautio, J.; Kärkkäinen, J.; Sloan, K. B. Prodrugs - Recent Approvals and a Glimpse of the Pipeline. *Eur. J. Pharm. Sci.* **2017**, *109*, 146–161.
- (28) Walther, R.; Rautio, J.; Zelikin, A. N. Prodrugs in Medicinal Chemistry and Enzyme Prodrug Therapies. *Adv. Drug Delivery Rev.* **2017**, *118*, 65–77.
- (29) Rautio, J.; Meanwell, N. A.; Di, L.; Hageman, M. J. The Expanding Role of Prodrugs in Contemporary Drug Design and Development. *Nat. Rev. Drug Discovery* **2018**, *17*, 559–587.
- (30) Ghosh, K.; Mazumder Tagore, D.; Anumula, R.; Lakshmaiah, B.; Kumar, P. P. B. S.; Singaram, S.; Matan, T.; Kallipatti, S.; Selvam, S.; Krishnamurthy, P.; Ramarao, M. Crystal Structure of Rat Intestinal Alkaline Phosphatase - Role of Crown Domain in Mammalian Alkaline Phosphatases. *J. Struct. Biol.* **2013**, *184*, 182–192.
- (31) Subramanian, M.; Paruchury, S.; Pratap Singh, S.; Arla, R.; Pahwa, S.; Jana, S.; Katnapally, P.; Yoganand, V.; Lakshmaiah, B.; Mazumder Tagore, D.; Ghosh, K.; Marathe, P.; Mandlekar, S. Characterization of Recombinantly Expressed Rat and Monkey Intestinal Alkaline Phosphatases: In Vitro Studies and In Vivo Correlations. *Drug Metab. Dispos.* **2013**, *41*, 1425–1432.
- (32) Yang, Y.-h.; Aloysius, H.; Inoyama, D.; Chen, Y.; Hu, L.-q. Enzyme-Mediated Hydrolytic Activation of Prodrugs. *Acta Pharm. Sin. B* **2011**, *1*, 143–159.
- (33) Riggs-Sauthier, J. Water Soluble Non-Peptidic Oligomer-Lipophilic Moieties-Protease Inhibitor Conjugates, Especially Containing Atazanavir and Tipranavir as the Protease Inhibitors, Their Preparation, Pharmacokinetics and Anti-HIV-1 Agents. WO 2010144869 A2, 2010.
- (34) Dhareshwar, S. S.; Stella, V. J. Your Prodrug Releases Formaldehyde: Should You be Concerned? No! *J. Pharm. Sci.* **2008**, *97*, 4184–4193.
- (35) Yamada, K.; Kato, K.; Nagase, H.; Hirata, Y. Protection of Tertiary Hydroxyl Groups as Methylthiomethyl Ethers. *Tetrahedron Lett.* **1976**, *17*, 65–66.
- (36) Huttunen, K. M.; Rautio, J. Prodrugs - an Efficient Way to Breach Delivery and Targeting Barriers. *Curr. Top. Med. Chem.* **2011**, *11*, 2265–2287.
- (37) Larson, K. B.; Wang, K.; Delille, C.; Otofokun, I.; Acosta, E. P. Pharmacokinetic Enhancers in HIV Therapeutics. *Clin. Pharmacokinetics.* **2014**, *53*, 865–872.
- (38) Vig, B. S.; Huttunen, K. M.; Laine, K.; Rautio, J. Amino Acids as Promoiety in Prodrug Design and Development. *Adv. Drug Delivery Rev.* **2013**, *65*, 1370–1385.
- (39) Krečmerová, M. Amino Acid Ester Prodrugs of Nucleoside and Nucleotide Antivirals. *Mini-Rev. Med. Chem.* **2017**, *17*, 818–833.
- (40) Murakami, T. A Mini-Review: Usefulness of Transporter-Targeted Prodrugs in Enhancing Membrane Permeability. *J. Pharm. Sci.* **2016**, *105*, 2515–2526.
- (41) Roche, D.; Greiner, J.; Aubertin, A.-M.; Vierling, P. Synthesis and in vitro Biological Evaluation of Valine-Containing Prodrugs Derived From Clinically Used HIV-Protease Inhibitors. *Eur. J. Med. Chem.* **2008**, *43*, 1506–1518.
- (42) Wang, Z.; Pal, D.; Mitra, A. K. Stereoselective Evasion of P-Glycoprotein, Cytochrome P450 3A, and Hydrolases by Peptide Prodrug Modification of Saquinavir. *J. Pharm. Sci.* **2012**, *101*, 3199–3213.
- (43) de Oliveira, M. P.; Olivier, J.-C.; Pariat, C.; Roche, D.; Greiner, J.; Vierling, P.; Couet, W. Investigation of Oral Bioavailability and Brain Distribution of the Ind(8)-Val Conjugate of Indinavir in Rodents. *J. Pharm. Pharmacol.* **2005**, *57*, 453–458.
- (44) Agarwal, S.; Boddu, S. H. S.; Jain, R.; Samanta, S.; Pal, D.; Mitra, A. K. Peptide Prodrugs: Improved Oral Absorption of Lopinavir, a HIV Protease Inhibitor. *Int. J. Pharm.* **2008**, *359*, 7–14.
- (45) Lai, L.; Xu, Z.; Zhou, J.; Lee, K.-D.; Amidon, G. L. Molecular Basis of Prodrug Activation by Human Valacyclovirase, an α -Amino Acid Ester Hydrolase. *J. Biol. Chem.* **2008**, *283*, 9318–9327.
- (46) Gaucher, B.; Rouquayrol, M.; Roche, D.; Greiner, J.; Aubertin, A.-M.; Vierling, P. Prodrugs of HIV Protease Inhibitors-Saquinavir, Indinavir and Nelfinavir-Derived from Diglycerides or Amino Acids: Synthesis, Stability and Anti-HIV Activity. *Org. Biomol. Chem.* **2004**, *2*, 345–357.
- (47) Rouquayrol, M.; Gaucher, B.; Roche, D.; Greiner, J.; Vierling, P. Transepithelial Transport of Prodrugs of the HIV Protease Inhibitors Saquinavir, Indinavir, and Nelfinavir Across Caco-2 Cell Monolayers. *Pharm. Res.* **2002**, *19*, 1704–1712.
- (48) Usansky, H. H.; Hu, P.; Sinko, P. J. Differential Roles of P-Glycoprotein, Multidrug Resistance-Associated Protein 2, and CYP3A on Saquinavir Oral Absorption in Sprague-Dawley Rats. *Drug Metab. Dispos.* **2008**, *36*, 863–869.

- (49) Gong, J.; Gan, J.; Caceres-Cortes, J.; Christopher, L. J.; Arora, V.; Masson, E.; Williams, D.; Pursley, J.; Allentoff, A.; Lago, M.; Tran, S. B.; Iyer, R. A. Metabolism and Disposition of [¹⁴C]Brivanib Alaninate after Oral Administration to Rats, Monkeys, and Humans. *Drug Metab. Dispos.* **2011**, *39*, 891–903.
- (50) Cai, Z.-w.; Zhang, Y.; Borzilleri, R. M.; Qian, L.; Barbosa, S.; Wei, D.; Zheng, X.; Wu, L.; Fan, J.; Shi, Z.; Wautlet, B. S.; Mortillo, S.; Jeyaseelan, R.; Kukral, D. W.; Kamath, A.; Marathe, P.; D'Arienzo, C.; Derbin, G.; Barrish, J. C.; Robl, J. A.; Hunt, J. T.; Lombardo, L. J.; Fargnoli, J.; Bhide, R. S. Discovery of Brivanib Alaninate ((S)-((R)-1-(4-(4-Fluoro-2-methyl-1H-indol-5-yloxy)-5-methylpyrrolo[2,1-f]-[1,2,4]triazin-6-yloxy)propan-2-yl)2-aminopropanoate), A Novel Prodrug of Dual Vascular Endothelial Growth Factor Receptor-2 and Fibroblast Growth Factor Receptor-1 Kinase Inhibitor (BMS-540215). *J. Med. Chem.* **2008**, *51*, 1976–1980.
- (51) Bou-Chacra, N.; Melo, K. J. C.; Morales, I. A. C.; Stippler, E. S.; Kesisoglou, F.; Yazdani, M.; Löbenberg, R. Evolution of Choice of Solubility and Dissolution Media After Two Decades of Biopharmaceutical Classification System. *AAPS J* **2017**, *19*, 989–1001.
- (52) Wang, J.; Yadav, V.; Smart, A. L.; Tajiri, S.; Basit, A. W. Toward Oral Delivery of Biopharmaceuticals: an Assessment of the Gastrointestinal Stability of 17 Peptide Drugs. *Mol. Pharm.* **2015**, *12*, 966–973.
- (53) Parrish, K. E.; Mao, J.; Chen, J.; Jaochico, A.; Ly, J.; Ho, Q.; Mukadam, S.; Wright, M. In Vitro and in Vivo Characterization of CYP Inhibition by 1-Aminobenzotriazole in Rats. *Biopharm. Drug Dispos.* **2016**, *37*, 200–211.
- (54) Vockley, J.; Andersson, H. C.; Antshel, K. M.; Braverman, N. E.; Burton, B. K.; Frazier, D. M.; Mitchell, J.; Smith, W. E.; Thompson, B. H.; Berry, S. A. Phenylalanine Hydroxylase Deficiency: Diagnosis and Management Guideline. *Genet. Med.* **2014**, *16*, 188–200.
- (55) Stappaerts, J.; Brouwers, J.; Annaert, P.; Augustijns, P. In Situ Perfusion in Rodents to Explore Intestinal Drug Absorption: Challenges and Opportunities. *Int. J. Pharm.* **2015**, *478*, 665–681.
- (56) Zhang, D.; Chando, T. J.; Everett, D. W.; Patten, C. J.; Dehal, S. S.; Humphreys, W. G. In vitro Inhibition of UDP Glucuronosyltransferases by Atazanavir and Other HIV Protease Inhibitors and the Relationship of This Property to In Vivo Bilirubin Glucuronidation. *Drug Metab. Dispos.* **2005**, *33*, 1729–1739.
- (57) Gammal, R.; Court, M.; Haidar, C.; Iwuchukwu, O.; Gaur, A.; Alvarelos, M.; Guillemette, C.; Lennox, J.; Whirl-Carrillo, M.; Brummel, S.; Ratain, M.; Klein, T.; Schackman, B.; Caudle, K.; Haas, D. Clinical Pharmacogenetics Implementation Consortium (CPIC) Guideline for UGT1A1 and Atazanavir Prescribing. *Clin. Pharmacol. Ther.* **2016**, *99*, 363–369.
- (58) Wang, B.-C.; Wang, L.-J.; Jiang, B.; Wang, S.-Y.; Wu, N.; Li, X.-Q.; Shi, D.-Y. Application of Fluorine in Drug Design During 2010–2015 Years: A Mini-Review. *Mini-Rev. Med. Chem.* **2017**, *17*, 683–692.
- (59) Ojima, I. Strategic Incorporation of Fluorine into Taxoid Anticancer Agents for Medicinal Chemistry and Chemical Biology Studies. *J. Fluorine Chem.* **2017**, *198*, 10–23.
- (60) Gillis, E. P.; Eastman, K. J.; Hill, M. D.; Donnelly, D. J.; Meanwell, N. A. Applications of Fluorine in Medicinal Chemistry. *J. Med. Chem.* **2015**, *58*, 8315–8359.
- (61) Meanwell, N. A. Fluorine and Fluorinated Motifs in the Design and Application of Biososteres for Drug Design. *J. Med. Chem.* **2018**, *61*, 5822–5880.
- (62) Ritchie, T. J.; Macdonald, S. J. F. Physicochemical Descriptors of Aromatic Character and Their Use in Drug Discovery. *J. Med. Chem.* **2014**, *57*, 7206–7215.
- (63) Pelletier, J. C.; Chen, S.; Bian, H.; Shah, R.; Smith, G. R.; Wrobel, J. E.; Reitz, A. B. Dipeptide Prodrugs of the Glutamate Modulator Riluzole. *ACS Med. Chem. Lett.* **2018**, *9*, 752–756.
- (64) Gomes, P.; Vale, N.; Moreira, R. Cyclization-Activated Prodrugs. *Molecules* **2007**, *12*, 2484–2506.
- (65) Santos, C.; Mateus, M. L.; Santos, A. P.; Moreira, R.; de Oliveira, E.; Gomes, P. Cyclization-Activated Prodrugs. Synthesis, Reactivity and Toxicity of Dipeptide Esters of Paracetamol. *Bioorg. Med. Chem. Lett.* **2005**, *15*, 1595–1598.
- (66) Meibom, D.; Albrecht-Küpper, B.; Diedrichs, N.; Hübsch, W.; Kast, R.; Krämer, T.; Krenz, U.; Lerchen, H.-G.; Mittendorf, J.; Nell, P. G.; Süßmeier, F.; Vakalopoulos, A.; Zimmermann, K. Neladenoson Bialanate Hydrochloride: A Prodrug of a Partial Adenosine A1 Receptor Agonist for the Chronic Treatment of Heart Diseases. *ChemMedChem* **2017**, *12*, 728–737.
- (67) Santos, C. R.; Capela, R.; Pereira, C. S. G. P.; Valente, E.; Gouveia, L.; Pannecouque, C.; De Clercq, E.; Moreira, R.; Gomes, P. Structure-Activity Relationships for Dipeptide Prodrugs of Acyclovir: Implications for Prodrug Design. *Eur. J. Med. Chem.* **2009**, *44*, 2339–2346.
- (68) Pérez-Picaso, L.; Escalante, J.; Olivo, H.; Rios, M. Y. Efficient Microwave Assisted Syntheses of 2,5-Diketopiperazines in Aqueous Media. *Molecules* **2009**, *14*, 2836–2849.
- (69) Robillard, K. R.; Chan, G. N. Y.; Zhang, G.; la Porte, W.; Bendayan, R. Role of P-Glycoprotein in the Distribution of the HIV Protease Inhibitor Atazanavir in the Brain and Male Genital Tract. *Antimicrob. Agents Chemother.* **2014**, *58*, 1713–1722.
- (70) Kis, O.; Walmsley, S. L.; Bendayan, R. In vitro and In situ Evaluation of pH-Dependence of Atazanavir Intestinal Permeability and Interactions with Acid-Reducing Agents. *Pharm. Res.* **2014**, *31*, 2404–2419.